Error Analysis and Model Adaptivity for Flows in Gas Networks[*]

Jeroen J. Stolwijk and Volker Mehrmann

Abstract

In the simulation and optimization of natural gas flow in a pipeline network, a hierarchy of models is used that employs different formulations of the Euler equations. While the optimization is performed on piecewise linear models, the flow simulation is based on the one to three dimensional Euler equations including the temperature distributions. To decide which model class in the hierarchy is adequate to achieve a desired accuracy, this paper presents an error and perturbation analysis for a two level model hierarchy including the isothermal Euler equations in semilinear form and the stationary Euler equations in purely algebraic form. The focus of the work is on the effect of data uncertainty, discretization, and rounding errors in the numerical simulation of these models and their interaction. Two simple discretization schemes for the semilinear model are compared with respect to their conditioning and temporal stepsizes are determined for which a well-conditioned problem is obtained. The results are based on new componentwise relative condition numbers for the solution of nonlinear systems of equations. Moreover, the model error between the semilinear and the algebraic model is computed, the maximum pipeline length is determined for which the algebraic model can be used safely, and a condition is derived for which the isothermal model is adequate.

1 Introduction

Natural gas plays a crucial role in the energy supply of the world. It is sufficiently and readily available, it is traded, and it is storable. In Germany e.g., after oil, natural gas is the second most used energy supplier, with a total share of more than 20% of the energy consumption in 2015 [1]. The high demand for natural gas and the deregulation of the energy markets call for a reliable mathematical modeling, simulation, and optimization of the gas transport through existing pipeline networks.

In view of this demand,in the last decades considerable research on the simulation and optimization of gas networks has been performed, see e.g. [2, 3, 4, 5, 6, 7, 8, 9, 10, 11, 12, 13, 14], where different simulation models for the flow through a pipe or a network of pipes and compressor stations have been proposed. Since the simulation models are a key factor in optimization tools, adequate accuracy and high efficiency is very important. So, using error estimation, typically the grid is adapted in space and time and as a new component of the simulation process we will discuss the adaptation of the model within a model hierarchy. We will focus on the pure pipe flow, where the model hierarchy is easily constructed and where it can be used to find an appropriate trade-off between accuracy and computational complexity, see [15, 16, 17, 18].

It is well known, see e.g. [19, page 5], that the numerical solution of a computational problem contains errors from all or some of the following sources: modeling, discretization, iteration, data uncertainty, and rounding errors, see Figure 1 for a schematic overview. These errors should be balanced to achieve an adequate simulation result. We derive error estimates and a sensitivity analysis within the typical model hierarchy with respect to the discretization scheme, while also considering the iteration and rounding errors for the solution of the resulting nonlinear systems of equations. To demonstrate the new techniques and to keep the presentation simple we present a deterministic as well as statistical error and sensitivity analysis only for two specific components of the model hierarchy, a purely algebraic model and an isothermal semilinear model, but the analysis can be carried out also for more complex components in the model hierarchy. For these two models, model and discretization error estimators for an arbitrary cost functional have been derived in [17, 20]. However, the effect of data uncertainty and rounding errors on the solution of these two models has not been considered in the literature and is the main topic of this paper.

To estimate the errors, we perform a backward error analysis, see e.g. [19], and derive first order upper bounds as well as mean statistical estimates for the error in the solution due to data uncertainty, modeling, discretization, round-
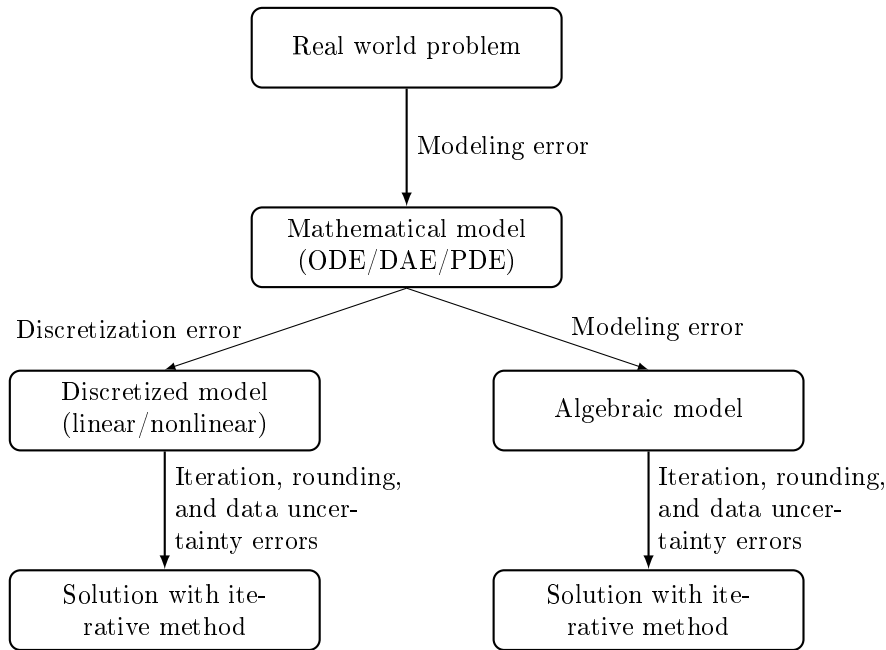
Figure 1: Overview of different error sources contained in the numerical simulation of a real world problem.

ing, and iteration errors. A perturbation analysis in which also higher order error terms are included usually leads to very pessimistic upper error bounds, see [21], and is therefore not considered. We derive componentwise condition numbers and, based on these, deterministic first order error bounds. The advantage of the componentwise relative condition number over the traditional normwise condition number for nonlinear systems is demonstrated.

This paper is organized as follows. Section 2 introduces different models that describe the gas flow through a pipeline. Section 3 gives a concise introduction into error analysis and conditioning. Moreover, several kinds of condition numbers are derived. Section 4 presents a sensitivity analysis for two different discretization schemes applied to the semilinear model and applies the derived condition numbers to the resulting nonlinear systems of equations. Moreover, the effect of rounding errors and the iteration error is investigated and the relative model error between the semilinear and the algebraic model is determined. In Section 5 both a theoretical worst case and a statistical mean error analysis for the stationary Euler equations in purely

algebraic form is presented. Some conclusions are given in Section 6.

2 The Model Hierarchy

As a model problem for the balanced error analysis in a model hierarchy, the gas flow through a pipeline is modeled via the one dimensional Euler equations that represent a system of nonlinear hyperbolic partial differential equations for the behavior of compressible, non-viscous fluids. The model consist of, see e.g. [22], the continuity equation, the impulse equation, and the energy equation, respectively,

$$\frac{\partial \rho}{\partial t} + \frac{\partial}{\partial x}(\rho v) = 0, \tag{1a}$$

$$\frac{\partial}{\partial t}(\rho v) + \frac{\partial}{\partial x}(p + \rho v^2) = -\frac{\lambda}{2D}\rho v|v| - g\rho h', \tag{1b}$$

$$\frac{\partial}{\partial t}\left(\rho(\frac{1}{2}v^2 + e)\right) + \frac{\partial}{\partial x}\left(\rho v(\frac{1}{2}v^2 + e) + pv\right) = -\frac{k_w}{D}(T - T_w). \tag{1c}$$

Moreover, the state equation for real gases is added, which is given by

$$p = R\rho T z(p, T). \tag{2}$$

In this system of equations the variables have the following physical meaning: ρ is the density of the gas, t is the time, v the velocity of the gas, x the space coordinate along the pipeline, p the pressure of the gas, λ the pipe friction coefficient, D the diameter of the pipeline, g the gravitational constant, h the height of the pipeline, $h'(x)$ the slope of the pipeline, c_v the volumetric heat capacity, $e = c_v T + gh$ the internal (thermal plus potential) energy, T the temperature of the gas, k_w the heat conductivity coefficient, T_w the wall temperature of the pipeline, and R the gas constant. Finally, $z(p, T)$ denotes the compressibility factor for which we use the model of the American Gas Association (AGA)

$$z(p, T) = 1 + 0.257\frac{p}{p_c} - 0.533\frac{pT_c}{p_cT}, \tag{3}$$

where p_c and T_c denote the pseudo-critical pressure and temperature, which provides a good approximation of z for pressures up to 70 bar [23, 24]. The full Euler equations (even in the one-dimensional case (1)) are mathematically quite involved and their numerical solution requires large computational effort. For this reason, in particular when the solution is part of an optimization procedure, usually several simplifications are made. Such simplifications are e.g. to use an approximate semilinear model as derived in subsection 2.1 or a purely algebraic model as considered in subsection 2.2.

2.1 Derivation of the Semilinear Isothermal Model

Starting from the full one dimensional Euler equations (1), to derive the isothermal model, the temperature $T = T_0$ is assumed to be constant within the pipeline, such that the energy equation (1c) can be dropped and the isothermal Euler equations (1a) and (1b) are obtained. According to the International Standard Metric Conditions for natural gas [25], the value $T_0 = 15.0\,°\text{C}$ (which is equal to $288\,\text{K}$) is taken for this constant temperature. Then, in the isothermal case, the compressibility factor z in the AGA model (3) only depends on p and we get

$$z(p) = 1 + \alpha p, \quad \text{with} \quad \alpha = \frac{0.257}{p_c} - 0.533\frac{T_c}{p_c T_0}. \tag{4}$$

If one also assumes that this compressibility factor $z(p) = z_0$ is constant in p, then one can use the average

$$z_0 = \frac{z(0) + z(70\,\text{bar})}{2} = 0.928$$

as its value. For constant temperature T_0 and compressibility factor z_0, the state equation for real gases (2) then reduces to

$$p(\rho) = RT_0 z_0 \rho. \tag{5}$$

If also the entropy of the gas is assumed to be constant, which is a reasonable assumption when the temperature of the gas is constant [17, page 7], then the speed of sound is given by $c = \sqrt{\partial p/\partial \rho}$, see also [22, Eq. (14.32)]. From (5) it follows that

$$c = \sqrt{RT_0 z_0} = \sqrt{p/\rho}. \tag{6}$$

Hence, we have $\rho = p/c^2$, and inserting this in (1b), the momentum equation can be rewritten as

$$\frac{\partial}{\partial t}(\rho v) + \frac{\partial}{\partial x}(p(1 + v^2/c^2)) = -\frac{\lambda}{2D}\rho v|v| - g\rho h'.$$

As further simplifications often the term v^2/c^2 is neglected in the case of small gas flow velocities v, see [26], and it is assumed that $h'(x) \equiv 0$, i.e., the pipeline is assumed to be (essentially) horizontal. These simplifications result in the *isothermal semilinear model* (see [17, 27])

$$\frac{\partial \rho}{\partial t} + \frac{\partial}{\partial x}(\rho v) = 0, \tag{7a}$$

$$\frac{\partial}{\partial t}(\rho v) + \frac{\partial p}{\partial x} = -\frac{\lambda}{2D}\rho v|v|. \tag{7b}$$

Introducing the *mass flow rate* $q = A\rho v$, with a constant cross-sectional area A, and using (6), system (7) may be rewritten in the form

$$\frac{\partial p}{\partial t} + \frac{c^2}{A}\frac{\partial q}{\partial x} = 0, \tag{8a}$$

$$\frac{\partial q}{\partial t} + A\frac{\partial p}{\partial x} = -\frac{\lambda c^2}{2DA}\frac{q|q|}{p}, \tag{8b}$$

$$q(x_R, t) = q_s(t), \tag{8c}$$

$$p(x_L, t) = p_s(t), \tag{8d}$$

where as boundary conditions the mass flow rate is prescribed by $q_s(t)$ at the *right-hand side of the pipeline* x_R and the pressure is prescribed by $p_s(t)$ at the *left-hand side of the pipeline* x_L.

When considering all these drastic model simplifications it has to be analyzed whether these perturbations in the model have a large effect on the simulation results.

2.2   Derivation of the Algebraic Model

Another simplified model (presented in an even more reduced form in [16]) is obtained by neglecting the terms $\frac{\partial}{\partial x}(\rho v^2)$, $\frac{\partial}{\partial x}(\rho v^3)$, and $\frac{\partial}{\partial t}(\rho v)$ in (1). This results in the model

$$\frac{\partial \rho}{\partial t} + \frac{\partial}{\partial x}(\rho v) = 0, \tag{9a}$$

$$\frac{\partial p}{\partial x} = -\frac{\lambda}{2D}\rho v|v| - g\rho h', \tag{9b}$$

$$\frac{\partial}{\partial t}(\rho e) + \frac{\partial}{\partial x}(\rho v e + pv) = -\frac{k_w}{D}(T - T_w). \tag{9c}$$

If, as further simplification, a stationary model is assumed, i.e., the time-derivatives $\frac{\partial}{\partial t}$ are set to zero, the pipeline is again assumed to be horizontal, i.e., $h' = 0$, and the compressibility factor z is set to be constant, then a set of ordinary differential equations is obtained, which can be solved analytically via

$$\hat{q} = \rho_{\text{in}} v_{\text{in}}, \tag{10a}$$

$$p(x) = \sqrt{p_{\text{in}}^2 - \frac{\lambda c^2}{2r}\rho v|\rho v|(x - x_0)}, \tag{10b}$$

$$T(x) = (T_{\text{in}} - T_w)e^{-\frac{k_w}{Dc_v\rho v}(x - x_0)} + T_w. \tag{10c}$$

Here, $\hat{q} = \rho v$ is the mass flux, which is constant in space, ρ_{in} is the inlet density, v_{in} the inlet velocity, p_{in} the inlet pressure, c the constant speed of sound,

r the radius of the pipeline, x_0 the starting point of the pipeline, and T_{in} the inlet temperature. Equations (10) are referred to as the *temperature dependent algebraic model* of the one dimensional Euler equations. Again, an isothermal simplification is obtained by taking the temperature T constant. This leaves us with (10a) and (10b), which are referred to as the *isothermal algebraic model*. A detailed derivation of this model is given in [18]. In the optimization of natural gas networks, this nonlinear algebraic model is often further approximated by piecewise linear functions, see e.g. [28] and [29, page 115]. Although usually within the optimization methods the approximation accuracy by the piecewise linear approximations is controlled, the modeling error of the nonlinear algebraic model is usually not considered. If this modeling error is large, then the linear relaxation techniques used in the optimization methods inevitably lead to inaccurate results. This motivates our consideration of the model error in subsection 4.5.

The discussed model hierarchy is depicted schematically in Figure 2. We will analyze the errors in this model hierarchy, however, it should be clear that the analysis can be extended by considering all simplifications separately and by also starting from a more detailed original model.
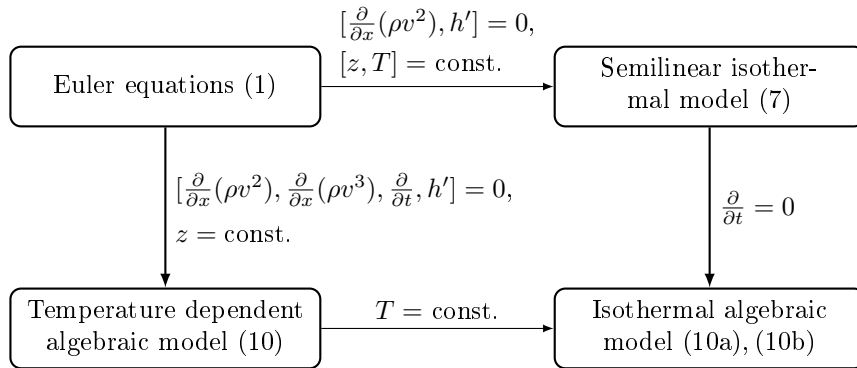
Figure 2: Two level model hierarchy for the simulation of flows in gas networks.

3 Error Analysis and Conditioning

The aim of *error analysis* is to construct an estimate or upper bound of the effect that modeling, rounding, data uncertainty, and discretization errors have on the solution of a given problem, see e.g. [30, 19, 31]. Rounding errors in the numerical computations due to floating point arithmetic can be interpreted as perturbations in the data using a backward error analysis, see [32]. We

investigate the data uncertainty error by means of a sensitivity analysis. A deterministic perturbation analysis, as given in subsection 3.1, results in a first order upper error bound, which can possibly be very pessimistic for certain input parameter values. Therefore, it is important to compare this upper bound with an average error estimate, which can be obtained using a statistical analysis as described in subsection 3.2.

3.1 Deterministic Perturbation Analysis

The term *condition number* is used to describe the sensitivity of problems to uncertainties in the input parameters [31]. Using the classical concepts of backward and forward error, we have the rule of thumb [19]

$$\text{forward error} \leqdot \text{condition number} \times \text{backward error},$$

with $\leqdot$ meaning "less than or equal to except for higher order terms". It insightfully shows that despite of a small backward error (which is often given by the residual), a problem can have a large forward error due to a high condition number. Formal definitions for normwise and componentwise condition numbers are given in e.g. [33].

Suppose that the solution of a problem is obtained by evaluating the differentiable function of a single variable $f(d)$. Denoting the derivative of f with respect to d by $f'(d)$, then the quantity [19]

$$\kappa_{\mathrm{rel}}(f; d) = \left| \frac{d\, f'(d)}{f(d)} \right|,$$

with $|\,.\,|$ denoting the absolute value, is the *relative condition number* of f and it measures, for small perturbations Δd, the relative change in the output for a given relative change in the input. On the other hand, if the solution of a problem is obtained by evaluating a differentiable function of several variables $f(\boldsymbol{d})$ with $\boldsymbol{d} \in \mathbb{R}^n$, then, using a first order Taylor series expansion, we have

$$\frac{f(\boldsymbol{d} + \boldsymbol{\Delta d}) - f(\boldsymbol{d})}{f(\boldsymbol{d})} \doteq \sum_{i=1}^{n} \frac{\partial f(\boldsymbol{d})}{\partial d_i} \frac{d_i}{f(\boldsymbol{d})} \frac{\Delta d_i}{d_i},$$

where $\doteq$ denotes a first order approximation, cf. [33, page 28]. Taking the absolute value results in the first order upper bounds

$$\frac{|f(\boldsymbol{d} + \boldsymbol{\Delta d}) - f(\boldsymbol{d})|}{|f(\boldsymbol{d})|} \leqdot \sum_{i=1}^{n} \left| \frac{\partial f(\boldsymbol{d})}{\partial d_i} \frac{d_i}{f(\boldsymbol{d})} \right| \frac{|\Delta d_i|}{|d_i|}$$

$$\leq \sum_{i=1}^{n} \left| \frac{\partial f(\boldsymbol{d})}{\partial d_i} \frac{d_i}{f(\boldsymbol{d})} \right| \cdot \max_{i} \frac{|\Delta d_i|}{|d_i|},$$

such that the quantities, cf. [21],

$$\kappa_{\mathrm{rel}}(f; d_i) = \left| \frac{\partial f(\boldsymbol{d})}{\partial d_i} \frac{d_i}{f(\boldsymbol{d})} \right|, \quad i = 1, \ldots, n, \tag{11}$$

are the *individual relative condition numbers* of f with respect to d_i and the quantity

$$\kappa_{\mathrm{rel}}(f; \boldsymbol{d}) = \sum_{i=1}^{n} \left| \frac{\partial f(\boldsymbol{d})}{\partial d_i} \frac{d_i}{f(\boldsymbol{d})} \right| = \sum_{i=1}^{n} \kappa_{\mathrm{rel}}(f; d_i) \tag{12}$$

is the relative condition number of f with respect to $\boldsymbol{d}$.

For systems of nonlinear equations, normwise relative condition numbers were first studied in [34], and the results are extended and summarized in [19]. We develop componentwise condition numbers for nonlinear systems of equations

$$F(\boldsymbol{x}; \boldsymbol{d}) = 0, \tag{13}$$

where $F : D_{\boldsymbol{x}} \times D_{\boldsymbol{d}} \to \mathbb{R}^m$ with $D_{\boldsymbol{x}} \times D_{\boldsymbol{d}}$ an open subset of $\mathbb{R}^m \times \mathbb{R}^n$. In the following we assume that $F \in C^{1,1}$, i.e., it is (at least once) continuously differentiable with respect to both $\boldsymbol{x}$ and $\boldsymbol{d}$. Given a solution $\boldsymbol{x}^* \in \mathbb{R}^m$ we are interested in the sensitivity of $\boldsymbol{x}^*$ with respect to perturbations in the data vector $\boldsymbol{d} \in \mathbb{R}^n$, i.e., we are interested in the condition number $\kappa_{\mathrm{rel}}(\boldsymbol{x}^*; \boldsymbol{d})$ of $\boldsymbol{x}^*$ with respect to perturbations $\tilde{\boldsymbol{d}}$ in the data $\boldsymbol{d}$. So instead of (13) one solves the problem

$$F(\tilde{\boldsymbol{x}}; \tilde{\boldsymbol{d}}) = 0, \tag{14}$$

and we determine a relation between the norms $||\tilde{\boldsymbol{x}}^* - \boldsymbol{x}^*||$ for the solutions $\tilde{\boldsymbol{x}}^*, \boldsymbol{x}^*$ and the deviation in the data $||\tilde{\boldsymbol{d}} - \boldsymbol{d}||$, where the norm $|| \cdot ||$ should be chosen such that it fits the problem [34, page 374]. The first order term in the Taylor series expansion gives

$$F(\tilde{\boldsymbol{x}}^*; \tilde{\boldsymbol{d}}) \doteq F(\boldsymbol{x}^*; \boldsymbol{d}) + F'_{\boldsymbol{x}}(\boldsymbol{x}^*; \boldsymbol{d})(\tilde{\boldsymbol{x}}^* - \boldsymbol{x}^*) + F'_{\boldsymbol{d}}(\boldsymbol{x}^*; \boldsymbol{d})(\tilde{\boldsymbol{d}} - \boldsymbol{d}), \tag{15}$$

where $F'_{\boldsymbol{x}}$ and $F'_{\boldsymbol{d}}$ denote the Jacobians of F with respect to $\boldsymbol{x}^*$ and $\boldsymbol{d}$, respectively. Since both $F(\boldsymbol{x}^*; \boldsymbol{d}) = 0$ and $F(\tilde{\boldsymbol{x}}^*; \tilde{\boldsymbol{d}}) = 0$, (15) can be rewritten as

$$F'_{\boldsymbol{x}}(\boldsymbol{x}^*; \boldsymbol{d})(\tilde{\boldsymbol{x}}^* - \boldsymbol{x}^*) \doteq -F'_{\boldsymbol{d}}(\boldsymbol{x}^*; \boldsymbol{d})(\tilde{\boldsymbol{d}} - \boldsymbol{d}). \tag{16}$$

If $F'_{\boldsymbol{x}}$ is invertible and bounded in $(\boldsymbol{x}^*; \boldsymbol{d})$, then we obtain that

$$||\tilde{\boldsymbol{x}}^* - \boldsymbol{x}^*|| \dot{\leq} ||F'_{\boldsymbol{x}}(\boldsymbol{x}^*; \boldsymbol{d})^{-1} F'_{\boldsymbol{d}}(\boldsymbol{x}^*; \boldsymbol{d})|| \, ||\tilde{\boldsymbol{d}} - \boldsymbol{d}||, \tag{17}$$

so that

$$\frac{||\tilde{\boldsymbol{x}}^* - \boldsymbol{x}^*||}{||\boldsymbol{x}^*||} \dot{\leq} \frac{||\boldsymbol{d}|| \, ||F'_{\boldsymbol{x}}(\boldsymbol{x}^*; \boldsymbol{d})^{-1} F'_{\boldsymbol{d}}(\boldsymbol{x}^*; \boldsymbol{d})||}{||\boldsymbol{x}^*||} \frac{||\tilde{\boldsymbol{d}} - \boldsymbol{d}||}{||\boldsymbol{d}||}, \tag{18}$$

where the matrix norm $||F'_{\boldsymbol{x}}(\boldsymbol{x}^*;\boldsymbol{d})^{-1}F'_{\boldsymbol{d}}(\boldsymbol{x}^*;\boldsymbol{d})||$ is the one induced by the vector norm. >From (17) and (18) it follows that the normwise absolute and relative condition numbers of the solution $\boldsymbol{x}^*$ with respect to the data $\boldsymbol{d}$ are given by

$$\kappa_{\mathrm{abs,n}}(\boldsymbol{x}^*;\boldsymbol{d}) = ||F'_{\boldsymbol{x}}(\boldsymbol{x}^*;\boldsymbol{d})^{-1}F'_{\boldsymbol{d}}(\boldsymbol{x}^*;\boldsymbol{d})|| \tag{19}$$

and, see [34, page 377] and [19, Eq. (25.11)],

$$\kappa_{\mathrm{rel,n}}(\boldsymbol{x}^*;\boldsymbol{d}) = \frac{||\boldsymbol{d}||\,||F'_{\boldsymbol{x}}(\boldsymbol{x}^*;\boldsymbol{d})^{-1}F'_{\boldsymbol{d}}(\boldsymbol{x}^*;\boldsymbol{d})||}{||\boldsymbol{x}^*||}, \tag{20}$$

respectively. Considering individual components, one can determine the sensitivity of the i-th component x_i^* of the solution vector $\boldsymbol{x}^*$ of the problem (13) with respect to small perturbations in the data vector $\boldsymbol{d}$. We rewrite (16) as

$$\tilde{\boldsymbol{x}}^* - \boldsymbol{x}^* \doteq -F'_{\boldsymbol{x}}(\boldsymbol{x}^*;\boldsymbol{d})^{-1}F'_{\boldsymbol{d}}(\boldsymbol{x}^*;\boldsymbol{d})(\tilde{\boldsymbol{d}}-\boldsymbol{d}). \tag{21}$$

For the i-th component $(\tilde{\boldsymbol{x}}^* - \boldsymbol{x}^*)_i$ of the vector $\tilde{\boldsymbol{x}}^* - \boldsymbol{x}^*$ we obtain

$$\begin{aligned}
(\tilde{\boldsymbol{x}}^* - \boldsymbol{x}^*)_i &\doteq - \left(F'_{\boldsymbol{x}}(\boldsymbol{x}^*;\boldsymbol{d})^{-1}F'_{\boldsymbol{d}}(\boldsymbol{x}^*;\boldsymbol{d})(\tilde{\boldsymbol{d}}-\boldsymbol{d}) \right)_i \\
&\doteq - \left(F'_{\boldsymbol{x}}(\boldsymbol{x}^*;\boldsymbol{d})^{-1}F'_{\boldsymbol{d}}(\boldsymbol{x}^*;\boldsymbol{d}) \right)_{i,:}(\tilde{\boldsymbol{d}}-\boldsymbol{d}),
\end{aligned} \tag{22}$$

where $M_{i,:}$ denotes the i-th row of the matrix M. Taking the absolute value and using the Cauchy-Schwarz inequality [35, page 107] result in first order upper bounds for the absolute and relative error

$$|\tilde{x}_i^* - x_i^*| \dot{\leq} \|\left(F'_{\boldsymbol{x}}(\boldsymbol{x}^*;\boldsymbol{d})^{-1}F'_{\boldsymbol{d}}(\boldsymbol{x}^*;\boldsymbol{d})\right)_{i,:}^T\|_2\|\tilde{\boldsymbol{d}}-\boldsymbol{d}\|_2, \tag{23}$$

$$\frac{|\tilde{x}_i^* - x_i^*|}{|x_i^*|} \dot{\leq} \frac{\|\boldsymbol{d}\|_2\|\left(F'_{\boldsymbol{x}}(\boldsymbol{x}^*;\boldsymbol{d})^{-1}F'_{\boldsymbol{d}}(\boldsymbol{x}^*;\boldsymbol{d})\right)_{i,:}^T\|_2}{|x_i^*|}\frac{\|\tilde{\boldsymbol{d}}-\boldsymbol{d}\|_2}{\|\boldsymbol{d}\|_2}. \tag{24}$$

It follows that the absolute and relative condition number of component x_i^* with respect to $\boldsymbol{d}$ are given by

$$\kappa_{\mathrm{abs}}(x_i^*;\boldsymbol{d}) = \|\left(F'_{\boldsymbol{x}}(\boldsymbol{x}^*;\boldsymbol{d})^{-1}F'_{\boldsymbol{d}}(\boldsymbol{x}^*;\boldsymbol{d})\right)_{i,:}^T\|_2, \tag{25}$$

$$\kappa_{\mathrm{rel}}(x_i^*;\boldsymbol{d}) = \frac{\|\boldsymbol{d}\|_2\|\left(F'_{\boldsymbol{x}}(\boldsymbol{x}^*;\boldsymbol{d})^{-1}F'_{\boldsymbol{d}}(\boldsymbol{x}^*;\boldsymbol{d})\right)_{i,:}^T\|_2}{|x_i^*|}. \tag{26}$$

Let us now consider, analogous to [36, Example 3.7], componentwise condition numbers in both the input and the output parameters. Since we are interested in the maximum componentwise error in the output parameters, we take the infinity norm in (21), which yields

$$\|\Delta\boldsymbol{x}^*\|_\infty \dot{\leq} \|F'_{\boldsymbol{x}}(\boldsymbol{x}^*;\boldsymbol{d})^{-1}F'_{\boldsymbol{d}}(\boldsymbol{x}^*;\boldsymbol{d})\|_\infty\|\Delta\boldsymbol{d}\|_\infty,$$

where $\Delta \boldsymbol{x}^* = \tilde{\boldsymbol{x}}^* - \boldsymbol{x}^*$ and $\Delta \boldsymbol{d} = \tilde{\boldsymbol{d}} - \boldsymbol{d}$. Thus, the componentwise absolute condition number is given by

$$\kappa_{\mathrm{abs,c}}(\boldsymbol{x}^*; \boldsymbol{d}) = \|F'_{\boldsymbol{x}}(\boldsymbol{x}^*; \boldsymbol{d})^{-1} F'_{\boldsymbol{d}}(\boldsymbol{x}^*; \boldsymbol{d})\|_\infty. \tag{27}$$

In order to derive the componentwise relative condition number, we define matrices $D_{\boldsymbol{x}^*} = \mathrm{diag}(x_i^*)$ and $D_{\boldsymbol{d}} = \mathrm{diag}(d_i)$, analogous to [36, Def. 3.1]. Then, (21) is equivalent to

$$D_{\boldsymbol{x}^*}^{-1} \Delta \boldsymbol{x}^* \doteq -D_{\boldsymbol{x}^*}^{-1} F'_{\boldsymbol{x}}(\boldsymbol{x}^*; \boldsymbol{d})^{-1} F'_{\boldsymbol{d}}(\boldsymbol{x}^*; \boldsymbol{d}) D_{\boldsymbol{d}} D_{\boldsymbol{d}}^{-1} \Delta \boldsymbol{d},$$

where we assume that all components of $\boldsymbol{x}^*$ and $\boldsymbol{d}$ are nonzero, such that the inverses $D_{\boldsymbol{x}^*}^{-1}$ and $D_{\boldsymbol{d}}^{-1}$ exist. Taking the infinity norm again yields

$$\|D_{\boldsymbol{x}^*}^{-1} \Delta \boldsymbol{x}^*\|_\infty \dot{\le} \|D_{\boldsymbol{x}^*}^{-1} F'_{\boldsymbol{x}}(\boldsymbol{x}^*; \boldsymbol{d})^{-1} F'_{\boldsymbol{d}}(\boldsymbol{x}^*; \boldsymbol{d}) D_{\boldsymbol{d}}\|_\infty \|D_{\boldsymbol{d}}^{-1} \Delta \boldsymbol{d}\|_\infty. \tag{28}$$

Hence, the *componentwise relative condition number* of $\boldsymbol{x}^*$ with respect to $\boldsymbol{d}$ is given by

$$\kappa_{\mathrm{rel,c}}(\boldsymbol{x}^*; \boldsymbol{d}) = \|D_{\boldsymbol{x}^*}^{-1} F'_{\boldsymbol{x}}(\boldsymbol{x}^*; \boldsymbol{d})^{-1} F'_{\boldsymbol{d}}(\boldsymbol{x}^*; \boldsymbol{d}) D_{\boldsymbol{d}}\|_\infty. \tag{29}$$

Note that by choosing the infinity norm in (20), we have the relation

$$\kappa_{\mathrm{rel,c}}(\boldsymbol{x}^*; \boldsymbol{d}) \le \kappa_{\mathrm{rel,n}}(\boldsymbol{x}^*; \boldsymbol{d}) \tag{30}$$

due to the sub-multiplicativity of the infinity norm. Surprisingly, the componentwise relative condition number (29) for general nonlinear problems (13) has not been formulated in the literature before. E.g., in [33, Example 2.17], [36, Example 3.7] the componentwise relative condition number for the more specific nonlinear system $F(\boldsymbol{x}) = \boldsymbol{d}$ is derived. In [19, 34] only the normwise relative condition number for nonlinear system (13) is given. We note that the amount of literature considering the conditioning of general nonlinear systems is relatively small. This observation is also made in [19, page 468].

Remark. *If the nonlinear system (13) is solved using (a variant of) the Newton method, then in each Newton iteration the linear system*

$$F'(\boldsymbol{x}_j) \Delta \boldsymbol{x}_j = -F(\boldsymbol{x}_j), \tag{31}$$

has to be solved, where $\Delta \boldsymbol{x}_j = \boldsymbol{x}_{j+1} - \boldsymbol{x}_j$. It is shown in [34] that the data uncertainty error in $\boldsymbol{x}^*$ depends on the sensitivity of the nonlinear system (13) and not on the sensitivity of the linear system (31).

3.2 Statistical Perturbation Analysis

The condition number leads to a first order worst case perturbation bound. However, in practice, this error bound is rarely attained and the actual error could be much smaller. In order to have a more detailed description of the data uncertainty error, we therefore also compute average perturbation estimates by means of a statistical sensitivity analysis.

We perform this analysis by using the Univariate Reduced Quadrature (URQ) method, see [37]. This method presents a convenient trade-off between computational complexity and accuracy. In contrast to the large sample size that is required for a Monte Carlo Simulation (MCS), the URQ method only utilizes a sample size of $2n+1$, where n is the number of uncertain data components. This makes the URQ method computationally much less expensive than a MCS. The mean μ_{x_k} and the variance $\sigma_{x_k}^2$, $k = 1, \ldots, m$, of a solution component x_k in $\boldsymbol{x}$ are approximated in the URQ method using the quadrature formulas in [37, (20) and (21)]. We use the factor

$$\phi(\boldsymbol{x}; \boldsymbol{d}) = \frac{\max_k \sigma_{x_k}/\mu_{x_k}}{\max_i \sigma_{d_i}/\mu_{d_i}} \tag{32}$$

as a statistical measure for the average amplification of the uncertainties in the data d_i, $i = 1, \ldots, n$.

Having established normwise and componentwise condition numbers for general nonlinear systems of equations as well as an average uncertainty amplification measure, in the next sections we apply these results to study the sensitivity of the two classes of Euler equations with respect to perturbations in the data.

4   Error Analysis for the Semilinear Isothermal Model

In this section, an error analysis is performed for the isothermal Euler equations in semilinear form, called the *semilinear model.* Subsections 4.1 and 4.2 discuss two simple discretization schemes applied to the semilinear model (7). These simple discretization schemes, here called the *1S-scheme* and the *MP-scheme*, are typically used in the optimization of large gas networks, see [9, 38]. A theoretical worst case and a statistical mean sensitivity analysis for both systems is presented in subsection 4.3. A rounding and iteration error analysis for the two resulting nonlinear systems is contained in subsection 4.4. Finally, a first order upper bound for the relative model error between the semilinear and the algebraic model is derived in subsection 4.5.

4.1 Discretization using a One-Sided Evaluation

For notational convenience, we consider one space interval $[x_L, x_R]$ as a piece of length H of a pipeline and discretize system (8) first in space. There are many different possibilities to obtain such a discretization. Here, we approximate the space derivative by

$$\frac{\partial q}{\partial x} \approx \frac{q(x_R, t) - q(x_L, t)}{H}. \tag{33}$$

Furthermore, we use the evaluation $p(x_R, t)$ as an approximation of $p(x, t)$ and $q(x, t) \approx q(x_L, t)$. Inserting the boundary conditions (8c), (8d) into (8a), (8b) results in a system of ordinary differential equations (ODEs), which is given by

$$\dot{p}(x_R, t) + \frac{c^2}{AH}\big(q_s(t) - q(x_L, t)\big) = 0,$$

$$\dot{q}(x_L, t) + \frac{A}{H}\big(p(x_R, t) - p_s(t)\big) = -\frac{\lambda c^2}{2DA} \frac{q(x_L, t)|q(x_L, t)|}{p(x_R, t)}.$$

Using the implicit Euler discretization scheme in time and introducing the vector $\boldsymbol{x}^i = [p(x_R, t_i), q(x_L, t_i)]^T$, yields the nonlinear system of equations

$$F_1(\boldsymbol{x}^i, \boldsymbol{d}) = \frac{1}{\tau}(x_1^i - x_1^{i-1}) + \frac{c^2}{AH}(q_s^i - x_2^i) = 0, \tag{34a}$$

$$F_2(\boldsymbol{x}^i, \boldsymbol{d}) = \frac{1}{\tau}(x_2^i - x_2^{i-1}) + \frac{A}{H}(x_1^i - p_s^i) + \frac{\lambda c^2}{2DA} \frac{x_2^i|x_2^i|}{x_1^i} = 0. \tag{34b}$$

Here, the (uncertain) data are collected in the vector

$$\boldsymbol{d} = [A, \lambda, D, c, p_s^i, q_s^i, x_1^{i-1}, x_2^{i-1}]^T. \tag{35}$$

These are the cross-sectional area A, the Darcy friction factor λ, the diameter D, the speed of sound c, the boundary conditions, and the solution of the previous time step $\boldsymbol{x}^{i-1}$. The first three parameters are uncertain because their values cannot be determined accurately for pipelines that lie deep in the ground for a long period of time. The speed of sound c within the gas is uncertain because the temperature T and the compressibility factor z are set to a constant in (6) and thus a modeling error is made. The boundary values are subject to measurement errors (or simulation errors when the pipeline is split into smaller pieces), and $\boldsymbol{x}^{i-1}$ is uncertain due to the accumulation of discretization errors, as well as the rounding and data uncertainty errors in the previous time steps. We call this discretization scheme the *1S-scheme* in the following. It is similar to the discretization in [9, 38]; the only difference is

that p and q are there both evaluated in x_R, given that the gas flows from x_L to x_R. Equations (34) define a two-dimensional nonlinear system with solution $\boldsymbol{x}^i$. The Jacobian $F'_{\boldsymbol{x}^i}(\boldsymbol{x}^i, \boldsymbol{d})$ of $F = [F_1, F_2]^T$ with respect to $\boldsymbol{x}^i$ is given by

$$F'_{\boldsymbol{x}^i}(\boldsymbol{x}^i, \boldsymbol{d}) = \begin{bmatrix} \frac{1}{\tau} & -\frac{c^2}{AH} \\ \frac{A}{H} - \frac{\lambda c^2}{2DA} \frac{x_2^i |x_2^i|}{(x_1^i)^2} & \frac{1}{\tau} + \frac{\lambda c^2}{DA} \frac{|x_2^i|}{x_1^i} \end{bmatrix}. \tag{36}$$

For the solution $\boldsymbol{x}^i$ of the nonlinear system (34) we use the Newton method, see e.g. [39], with stopping criterion $\|\boldsymbol{x}_j^i - \boldsymbol{x}_{j-1}^i\|_\infty \leq \text{tol}$. In our simulations that we present below we use $\text{tol} = 10^{-3}$, the concrete parameters values

$$\tau = 15\,\text{s}, \quad p_R^{i-1} = 5 \cdot 10^6\,\text{Pa}, \quad q_L^{i-1} = 300\,\text{kg s}^{-1}, \tag{37a}$$

$$c = \sqrt{RT_0 z_0} = \sqrt{518.3 \cdot 288.15 \cdot 0.928} = 372\,\text{m s}^{-1}, \text{see (6)}, \tag{37b}$$

$$H = 500\,\text{m}, \quad p_s^i = 5.07 \cdot 10^6\,\text{Pa}, \quad q_s^i = 302\,\text{kg s}^{-1}, \tag{37c}$$

$$A = 0.785\,\text{m}^2, \quad \lambda = 0.06, \quad D = 1\,\text{m}, \tag{37d}$$

and starting values $\boldsymbol{x}_0^i = [5 \cdot 10^6\,\text{Pa}, 300\,\text{kg s}^{-1}]^T$. These values result in an approximate solution $\boldsymbol{x}^i$ which is given by

$$\boldsymbol{x}^i = \begin{bmatrix} p_R^i \\ q_L^i \end{bmatrix} = \begin{bmatrix} 5.01 \cdot 10^6\,\text{Pa} \\ 3.03 \cdot 10^2\,\text{kg s}^{-1} \end{bmatrix}. \tag{38}$$

An important question is, how sensitive this solution is with respect to small perturbations in the uncertain data $\boldsymbol{d}$ in (35). To determine this sensitivity, the Jacobian of F with respect to $\boldsymbol{d}$ is computed, which is given by

$$F'_{\boldsymbol{d}}(\boldsymbol{x}^i, \boldsymbol{d}) = \begin{bmatrix} \frac{c^2}{A^2 H}(x_2^i - q_s^i) & \frac{1}{H}(x_1^i - p_s^i) - \frac{\lambda c^2}{2DA^2}\frac{x_2^i|x_2^i|}{x_1^i} \\ 0 & \frac{c^2}{2DA}\frac{x_2^i|x_2^i|}{x_1^i} \\ 0 & -\frac{\lambda c^2}{2D^2 A}\frac{x_2^i|x_2^i|}{x_1^i} \\ \frac{2c}{AH}(q_s^i - x_2^i) & \frac{\lambda c}{DA}\frac{x_2^i|x_2^i|}{x_1^i} \\ 0 & -\frac{A}{H} \\ \frac{c^2}{AH} & 0 \\ -\frac{1}{\tau} & 0 \\ 0 & -\frac{1}{\tau} \end{bmatrix}^T. \tag{39}$$

The results of the sensitivity analysis are presented in subsection 4.3.

4.2 Discretization using the Midpoint Rule

As an alternative space discretization of the system (8) we use the midpoint rule for the pressure $p(x,t)$ and the mass flow rate $q(x,t)$. For example, for $p(x,t)$ we obtain

$$p(x,t) \approx \frac{p(x_R,t) + p(x_L,t)}{2}.$$

Again, the boundary conditions (8c), (8d) are inserted into (8a), (8b). This results in the system of ODEs

$$\frac{1}{2}\dot{p}(x_R,t) + \frac{c^2}{AH}\big(q_s(t) - q(x_L,t)\big) + \frac{1}{2}\dot{p}_s(t) = 0,$$

$$\frac{1}{2}\dot{q}(x_L,t) + \frac{A}{H}\big(p(x_R,t) - p_s(t)\big) + \frac{1}{2}\dot{q}_s(t)$$

$$+ \frac{\lambda c^2}{4DA}\frac{\big(q_s(t) + q(x_L,t)\big)|q_s(t) + q(x_L,t)|}{p(x_R,t) + p_s(t)} = 0.$$

Using again the implicit Euler scheme for the time discretization yields the nonlinear system

$$F_1(\boldsymbol{x}^i, \boldsymbol{d}) = \frac{1}{\tau}(x_1^i - x_1^{i-1}) + \frac{2c^2}{AH}(q_s^i - x_2^i) + \dot{p}_s^i = 0, \tag{41a}$$

$$F_2(\boldsymbol{x}^i, \boldsymbol{d}) = \frac{1}{\tau}(x_2^i - x_2^{i-1}) + \frac{2A}{H}(x_1^i - p_s^i) + \dot{q}_s^i$$

$$+ \frac{\lambda c^2}{2DA}\frac{(q_s^i + x_2^i)|q_s^i + x_2^i|}{x_1^i + p_s^i} = 0, \tag{41b}$$

with data vector

$$\boldsymbol{d} = [A, \lambda, D, c, p_s^i, q_s^i, \dot{p}_s^i, \dot{q}_s^i, x_1^{i-1}, x_2^{i-1}]^T. \tag{42}$$

We call this discretization scheme the *MP-scheme*. It is equivalent to the implicit box scheme in [40]. The Jacobian $F'_{\boldsymbol{x}^i}$ of $F = [F_1, F_2]^T$ with respect to $\boldsymbol{x}^i$ in this case is given by

$$F'_{\boldsymbol{x}^i}(\boldsymbol{x}^i, \boldsymbol{d}) = \begin{bmatrix} \frac{1}{\tau} & -\frac{2c^2}{AH} \\ \frac{2A}{H} - \frac{\lambda c^2}{2DA}\frac{(q_s^i + x_2^i)|q_s^i + x_2^i|}{(x_1^i + p_s^i)^2} & \frac{1}{\tau} + \frac{\lambda c^2}{DA}\frac{|q_s^i + x_2^i|}{x_1^i + p_s^i} \end{bmatrix}. \tag{43}$$

We again use the Newton method for the solution $\boldsymbol{x}^i$ of (41) with stopping criterion $\|\boldsymbol{x}_j^i - \boldsymbol{x}_{j-1}^i\|_\infty \leq \text{tol}$. For the numerical simulations presented below we use the parameter values (37),

$$\dot{p}_s^i = 100, \quad \dot{q}_s^i = 0.05, \tag{44}$$

and the starting values $\boldsymbol{x}_0^i = [5 \cdot 10^6\,\mathrm{Pa}, 300\,\mathrm{kg\,s^{-1}}]^T$. This results in an approximate solution $\boldsymbol{x}^i$ given by

$$\boldsymbol{x}^i = \begin{bmatrix} p_R^i \\ q_L^i \end{bmatrix} = \begin{bmatrix} 5.01 \cdot 10^6\,\mathrm{Pa} \\ 3.03 \cdot 10^2\,\mathrm{kg\,s^{-1}} \end{bmatrix}. \tag{45}$$

In order to determine the sensitivity of $\boldsymbol{x}^i$ with respect to perturbations in the data, the Jacobian of the function F with respect to $\boldsymbol{d}$ in (42) is calculated as

$$F_{\boldsymbol{d}}'(\boldsymbol{x}^i, \boldsymbol{d}) = \begin{bmatrix} \frac{2c^2}{A^2 H}\left(x_2^i - q_s^i\right) & \frac{2}{H}\left(x_1^i - p_s^i\right) - \frac{\lambda c^2}{2DA^2}\frac{(q_s^i + x_2^i)|q_s^i + x_2^i|}{x_1^i + p_s^i} \\ 0 & \frac{c^2}{2DA}\frac{(q_s^i + x_2^i)|q_s^i + x_2^i|}{x_1^i + p_s^i} \\ 0 & -\frac{\lambda c^2}{2D^2 A}\frac{(q_s^i + x_2^i)|q_s^i + x_2^i|}{x_1^i + p_s^i} \\ \frac{4c}{AH}\left(q_s^i - x_2^i\right) & \frac{\lambda c}{DA}\frac{(q_s^i + x_2^i)|q_s^i + x_2^i|}{x_1^i + p_s^i} \\ 0 & -\frac{2A}{H} - \frac{\lambda c^2}{2DA}\frac{(q_s^i + x_2^i)|q_s^i + x_2^i|}{(x_1^i + p_s^i)^2} \\ \frac{2c^2}{AH} & \frac{\lambda c^2}{DA}\frac{|q_s^i + x_2^i|}{x_1^i + p_s^i} \\ 1 & 0 \\ 0 & 1 \\ -\frac{1}{\tau} & 0 \\ 0 & -\frac{1}{\tau} \end{bmatrix}^T. \tag{46}$$

The sensitivity results are presented in subsection 4.3.

4.3   Sensitivity Analysis for the two Discretizations

This subsection contains both a worst case first order and a statistical mean sensitivity analysis for the 1S- and the MP- discretization scheme. Moreover, we show that the normwise condition number yields a too pessimistic upper error bound.

We use the Jacobians in $(36), (39), (43), (46)$ to calculate the individual condition numbers (26) of the components p_R^i and q_L^i of the solutions $\boldsymbol{x}^i$ in $(38), (45)$ with respect to perturbations in the uncertain data. Using the parameter values in $(37), (44)$ we obtain the results presented in Table 1. We find that the largest individual condition number is $\kappa_{\mathrm{rel}}(q_L^i; p_s^i)$ for both schemes. Moreover, one observes that the mass flow rate q_L^i is more sensitive to small perturbations in the parameters than the pressure p_R^i. We note that a scaling of the parameter values or using different units, e.g. by choosing the unit metric ton rather than kg, does not change the results.

Calculating the normwise relative condition numbers (20) of $\boldsymbol{x}^i$ with respect to $\boldsymbol{d}$ in (35), (42) for the 1S- and the MP-scheme with parameter values (37), (44) yields $\kappa_{\mathrm{rel,n}}^{\mathrm{1S}}(\boldsymbol{x}^i; \boldsymbol{d}) = 1.39 \cdot 10^6$, $\kappa_{\mathrm{rel,n}}^{\mathrm{MP}}(\boldsymbol{x}^i; \boldsymbol{d}) = 1.45 \cdot 10^6$. We find that these normwise condition numbers are at least three orders of magnitude larger than the individual condition numbers in Table 1. Hence, the normwise condition number considerably overestimates the sensitivity of the corresponding nonlinear root finding problem, i.e., it constitutes a very pessimistic upper bound. Considering also (30), this leads to the conclusion that it is more adequate to use the componentwise relative condition number in (29) in order to determine the sensitivity of $\boldsymbol{x}^i$ with respect to $\boldsymbol{d}$.

The componentwise condition numbers for the two different discretization schemes are calculated for spatial stepsizes $H \in [1, 1000\,\mathrm{m}]$ and for temporal stepsizes $\tau \in [10^{-2}, 30\,\mathrm{s}]$. The results are depicted in Figure 3. In order to get a more detailed description of the sensitivity of the nonlinear systems, we

Table 1: Individual relative condition numbers in (26) for the 1S- and the MP-scheme. The condition numbers are computed for the solution components p_R^i and q_L^i with respect to the uncertain input parameters $\boldsymbol{d}$ in (35), (42). The values in (37), (44) are used.

| | $\kappa_{\mathrm{rel}}^{\mathrm{1S}}$ | | $\kappa_{\mathrm{rel}}^{\mathrm{MP}}$ | |
	p_R^i	q_L^i	p_R^i	q_L^i
A	$2.30 \cdot 10^{-2}$	$7.65 \cdot 10^{-2}$	$2.40 \cdot 10^{-2}$	$4.07 \cdot 10^{-2}$
λ	$1.15 \cdot 10^{-2}$	$3.60 \cdot 10^{-2}$	$1.20 \cdot 10^{-2}$	$1.88 \cdot 10^{-2}$
D	$1.15 \cdot 10^{-2}$	$3.60 \cdot 10^{-2}$	$1.20 \cdot 10^{-2}$	$1.88 \cdot 10^{-2}$
c	$2.28 \cdot 10^{-2}$	$8.09 \cdot 10^{-2}$	$2.40 \cdot 10^{-2}$	$4.38 \cdot 10^{-2}$
p_s^i	$9.44 \cdot 10^{-1}$	2.94	1.00	1.57
q_s^i	$2.53 \cdot 10^{-2}$	$9.16 \cdot 10^{-1}$	$2.53 \cdot 10^{-2}$	$9.57 \cdot 10^{-1}$
$\dot{p}_s^i$	–	–	$6.23 \cdot 10^{-6}$	$4.58 \cdot 10^{-4}$
$\dot{q}_s^i$	–	–	$3.13 \cdot 10^{-6}$	$4.89 \cdot 10^{-6}$
p_R^{i-1}	$7.93 \cdot 10^{-2}$	2.87	$2.08 \cdot 10^{-2}$	1.53
q_L^{i-1}	$2.37 \cdot 10^{-3}$	$7.39 \cdot 10^{-3}$	$1.25 \cdot 10^{-3}$	$1.96 \cdot 10^{-3}$

also perform a statistical mean error analysis for the 1S- and the MP-scheme using the URQ method, see subsection 3.2. The relative standard deviations σ_{d_j}/μ_{d_j}, $j = 1, \ldots, n$, for the input parameters is set to 0.5% and the values in (37) are taken for the mean values μ_{d_j}. Subsequently, the relative standard deviations $\sigma_{x_k^i}/\mu_{x_k^i}$, $k = 1, 2$, of the solution $\boldsymbol{x}^i$ are computed. Factor $\phi(\boldsymbol{x}^i; \boldsymbol{d})$ in (32) is again calculated for $H \in [1, 1000\,\mathrm{m}]$ and $\tau \in [10^{-2}, 30\,\mathrm{s}]$. The results are depicted in Figure 4. We find that the differences between the mean uncertainty amplification factors ϕ and the first order worst case bounds in Figure 3 are relatively small. Furthermore, we observe in both figures that given H and τ, the sensitivity of the MP-scheme is smaller than that of the 1S-scheme. Using Figures 3 and 4 for a given discretization scheme, the spatial and temporal stepsizes H and τ can be chosen such that the sensitivity of the corresponding nonlinear system is low. Note that while reducing H and τ decreases the discretization error, it increases the sensitivity of the problem and thus both the error due to data uncertainty and the effect of rounding are amplified. Hence, a balance between the discretization and the data uncertainty error should be determined to find appropriate values for H and τ.
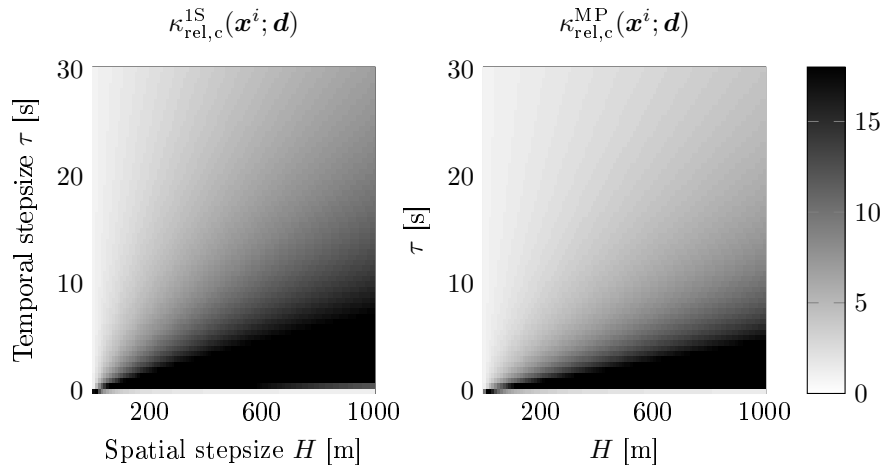

Figure 3: The componentwise relative condition numbers in (29) of the 1S-scheme (left) and the MP-scheme (right) as a function of the spatial and temporal stepsize. The condition number is computed for the solution $\boldsymbol{x}^i = [p_R^i, q_L^i]^T$ with respect to the uncertain data $\boldsymbol{d}$ in (35), (42). The numbers at the colorbar denote the values of $\kappa_{\mathrm{rel,c}}$.
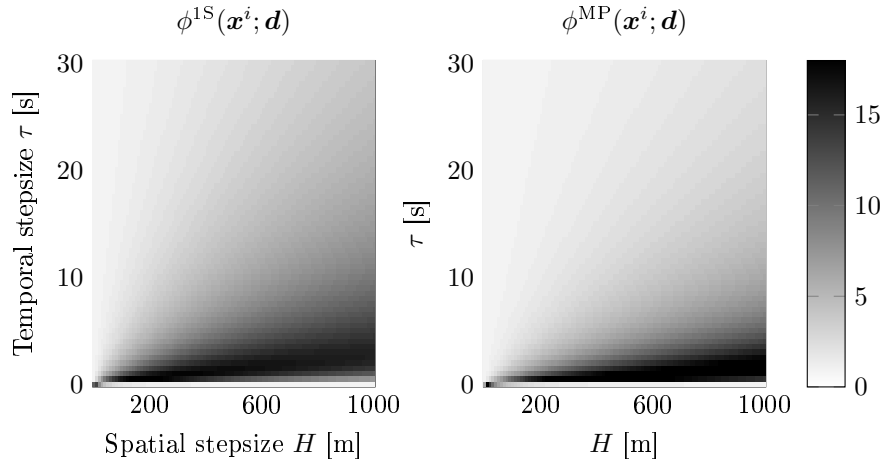
Figure 4: The mean uncertainty amplification factor $\phi(\boldsymbol{x}^i; \boldsymbol{d})$ in (32), calculated with the URQ method, for the 1S-scheme (left) and MP-scheme (right) as a function of H and τ. The values in (37) are taken for the mean values of the uncertain data. The numbers at the colorbar denote the values of ϕ.

4.4 Rounding and Iteration Error Analysis

In this subsection a first order upper bound for the rounding errors and the iteration error that are committed in the Newton method is derived. The result is applied to both the 1S- and the MP-scheme.

A rounding error analysis for the solution of the linear system (31) arising in the Newton method is presented in [41], together with a condition for which the intermediate solution $\boldsymbol{x}_j$ cannot be improved due to rounding errors, see [41, page 117]. If e_j is an upper bound for the rounding error $\|F(\boldsymbol{x}_j) - \tilde{F}(\boldsymbol{x}_j)\|$, where F is the exact function evaluation and $\tilde{F}$ is the computed function evaluation, then this condition is given by

$$\|\tilde{F}(\boldsymbol{x}_j)\| \leq e_j \quad \text{or} \quad \|\tilde{F}(\boldsymbol{x}_j)\| \geq \|\tilde{F}(\boldsymbol{x}_{j-1})\|. \tag{47}$$

In the following we assume that the first condition of (47) is satisfied before the second condition of (47). We define the set

$$\mathcal{S} := \{\boldsymbol{x} \mid \|\tilde{F}(\boldsymbol{x})\| \leq e_j\} \tag{48}$$

and assume that $\boldsymbol{x}^* \in \mathcal{S}$. Then, provided that the Jacobian of $\tilde{F}$ is invertible for all $\boldsymbol{x} \in \mathcal{S}$, it follows from the implicit function theorem that

$$
\begin{aligned}
\|\boldsymbol{x}_j - \boldsymbol{x}^*\| &\dot{\leq} \|[\tilde{F}'(\boldsymbol{x}_j)]^{-1}\| \, \|\tilde{F}(\boldsymbol{x}_j) - \tilde{F}(\boldsymbol{x}^*)\| \\
&\leq \|[\tilde{F}'(\boldsymbol{x}_j)]^{-1}\| \, (\|\tilde{F}(\boldsymbol{x}_j)\| + \|\tilde{F}(\boldsymbol{x}^*)\|) \\
&\leq \|[\tilde{F}'(\boldsymbol{x}_j)]^{-1}\| \, (\|\tilde{F}(\boldsymbol{x}_j)\| + e_j)
\end{aligned} \tag{49}
$$

for all $\boldsymbol{x}_j \in \mathcal{S}$. Let $\mathcal{B}(r)$ denote the ball with radius r around $\boldsymbol{x}^*$, i.e.,

$$
\mathcal{B}(r) = \{\boldsymbol{x} \mid \|\boldsymbol{x} - \boldsymbol{x}^*\| < r\}.
$$

It is well-known, see e.g. [39, Theorem 5.1.1], that under certain assumptions on the function F, e.g., Lipschitz continuity of F', there exists a $\xi > 0$ such that if $\boldsymbol{x}_j \in \mathcal{B}(\xi) \setminus \mathcal{S}$, then the Newton method converges quadratically, i.e., $\|\boldsymbol{x}_{j+1} - \boldsymbol{x}^*\| = O(\|\boldsymbol{x}_j - \boldsymbol{x}^*\|^2)$. This implies that

$$
\|\boldsymbol{x}_j - \boldsymbol{x}^*\| \leq \|\boldsymbol{x}_j - \boldsymbol{x}_{j+1}\| + O(\|\boldsymbol{x}_j - \boldsymbol{x}^*\|^2), \quad \text{for all} \ \ \boldsymbol{x}_j \in \mathcal{B}(\xi) \setminus \mathcal{S}. \tag{50}
$$

Thus, we have the following theorem.

Theorem 1. *Let a solution $\boldsymbol{x}_j$ of the nonlinear system arising in the gas flow simulation that is computed with the Newton method be given. Let η^{ri} denote the error in $\boldsymbol{x}_j$ both due to rounding errors in the solution of* (31) *and due to a preliminary stopping of the Newton iteration. Let e_j be an upper bound for the rounding error $\|F(\boldsymbol{x}_j) - \tilde{F}(\boldsymbol{x}_j)\|$. Suppose that $\mathcal{S} \subseteq \mathcal{B}(\xi)$ and $\boldsymbol{x}_j \in \mathcal{B}(\xi)$, then*

$$
\eta^{\mathrm{ri}} \dot{\leq} \begin{cases} \|[\tilde{F}'(\boldsymbol{x}_j)]^{-1}\| \, (\|\tilde{F}(\boldsymbol{x}_j)\| + e_j) & \text{if } \boldsymbol{x}_j \in \mathcal{S}, \\ \|\boldsymbol{x}_j - \boldsymbol{x}_{j+1}\| & \text{if } \boldsymbol{x}_j \in \mathcal{B}(\xi) \setminus \mathcal{S}. \end{cases} \tag{51}
$$

Proof. If $\boldsymbol{x}_j \in \mathcal{B}(\xi) \setminus \mathcal{S}$, then the Newton method converges quadratically despite rounding errors in the solution of (31), see [41, page 117]. Thus, η^{ri} is given by (50). On the other hand, if $\boldsymbol{x}_j \in \mathcal{S}$, then condition (47) is satisfied and we do not have convergence. An upper bound for η^{ri} is then given by (49). $\square$

To apply this result, we compute η^{ri} for the 1S- and the MP-scheme. For the 1S-scheme we may write

$$
\begin{aligned}
\tilde{F}_1(\boldsymbol{x}^i, \boldsymbol{d}) &= \frac{x_1^i - x_1^{i-1}}{\tau}(1 + 3\varepsilon) + \frac{c^2(q_s^i - x_2^i)}{AH}(1 + 6\varepsilon), \\
\tilde{F}_2(\boldsymbol{x}^i, \boldsymbol{d}) &= \frac{x_2^i - x_2^{i-1}}{\tau}(1 + 4\varepsilon) + \frac{A(x_1^i - p_s^i)}{H}(1 + 5\varepsilon) + \frac{\lambda c^2 x_2^i |x_2^i|}{2DAx_1^i}(1 + 8\varepsilon),
\end{aligned}
$$

where $|\varepsilon| \leq \mathbf{u}$ and $\mathbf{u}$ denotes the unit roundoff. Hence, we have

$$|F_1 - \tilde{F}_1| \leq \frac{|x_1^i - x_1^{i-1}|}{\tau} 3\mathbf{u} + \frac{c^2 |q_s^i - x_2^i|}{AH} 6\mathbf{u} =: \alpha^{1S},$$

$$|F_2 - \tilde{F}_2| \leq \frac{|x_2^i - x_2^{i-1}|}{\tau} 4\mathbf{u} + \frac{A|x_1^i - p_s^i|}{H} 5\mathbf{u} + \frac{\lambda c^2 (x_2^i)^2}{2DAx_1^i} 8\mathbf{u} =: \beta^{1S}$$

and, thus, $e_j^{1S} = \|[\alpha^{1S}, \beta^{1S}]^T\|$. For the MP-scheme we obtain

$$\tilde{F}_1 = \frac{x_1^i - x_1^{i-1}}{\tau}(1 + 4\varepsilon) + \frac{2c^2(q_s^i - x_2^i)}{AH}(1 + 7\varepsilon) + \dot{p}_s^i(1 + \varepsilon),$$

$$\tilde{F}_2 = \frac{x_2^i - x_2^{i-1}}{\tau}(1 + 5\varepsilon) + \frac{2A(x_1^i - p_s^i)}{H}(1 + 6\varepsilon) + \dot{q}_s^i(1 + 2\varepsilon)$$

$$+ \frac{\lambda c^2 (q_s^i + x_2^i)|q_s^i + x_2^i|}{2DA(x_1^i + p_s^i)}(1 + 11\varepsilon),$$

and, hence

$$|F_1 - \tilde{F}_1| \leq \frac{|x_1^i - x_1^{i-1}|}{\tau} 4\mathbf{u} + \frac{2c^2 |q_s^i - x_2^i|}{AH} 7\mathbf{u} + |\dot{p}_s^i|\mathbf{u} =: \alpha^{MP},$$

$$|F_2 - \tilde{F}_2| \leq \frac{|x_2^i - x_2^{i-1}|}{\tau} 5\mathbf{u} + \frac{2A|x_1^i - p_s^i|}{H} 6\mathbf{u} + |\dot{q}_s^i|2\mathbf{u}$$

$$+ \frac{\lambda c^2 (q_s^i + x_2^i)^2}{2DA(x_1^i + p_s^i)} 11\mathbf{u} =: \beta^{MP},$$

and $e_j^{MP} = \|[\alpha^{MP}, \beta^{MP}]^T\|$. Assuming the use of IEEE standard double precision arithmetic, such that $\mathbf{u} = 2.22 \cdot 10^{-16}$, see [19, page 39], and choosing the infinity norm, we obtain the following error estimates. For the 1S-scheme with the values in (37) and the solution $\boldsymbol{x}^i$ in (38) we have $e_j^{1S} = 1.16 \cdot 10^{-12}$ and $\|\tilde{F}(\boldsymbol{x}^i)\| = 1.74 \cdot 10^{-11}$. Thus, $\boldsymbol{x}^i$ is not an element of the set $\mathcal{S}$. We assume that $\boldsymbol{x}^i \in \mathcal{B}(\xi)$ such that we have $\eta^{ri} \dot{\leq} 1.56 \cdot 10^{-10}$. For the MP-scheme with the values in (44) and the solution $\boldsymbol{x}^i$ in (45) we have $e_j^{MP} = 1.73 \cdot 10^{-12}$ and $\|\tilde{F}(\boldsymbol{x}^i)\| = 2.22 \cdot 10^{-11}$. Hence, $\boldsymbol{x}^i$ again is not contained in $\mathcal{S}$. We again assume that $\boldsymbol{x}^i \in \mathcal{B}(\xi)$ such that we have $\eta^{ri} \dot{\leq} 7.82 \cdot 10^{-11}$. It can be concluded that for both schemes the rounding and iteration errors can be neglected in comparison with the data uncertainty error.

4.5   Modeling Error between the Semilinear and Algebraic Model

In this subsection we analyze the modeling error that is committed when the isothermal semilinear model (7) is simplified to the isothermal algebraic model (10a), (10b) that is obtained by assuming a stationary gas flow, see Figure 2.

We consider the semilinear and the algebraic model on the spatial interval $[0, L]$, with pipeline length L, and the temporal interval $[0, T]$. We define gridpoints (x_i, t^k), $i = 0, \dots, N$ and $k = 0, \dots, M$, with stepsizes $H = L/N$ and $\tau = T/M$. Let the solution of the semilinear model at the gridpoints be denoted by $\boldsymbol{y}^{\mathrm{sem}}(x_i, t^k)$, the solution of the discretized semilinear model with stepsizes H and τ at the gridpoints (x_i, t^k) be denoted by $\boldsymbol{y}_i^k(H, \tau)$, and the solution of the algebraic model at the gridpoints be denoted by $\boldsymbol{y}^{\mathrm{alg}}(x_i)$, with $\boldsymbol{y}(x, t) = [p(x, t), q(x, t)]^T$. We define the relative model error η^{m} between the semilinear and the algebraic model by

$$\eta^{\mathrm{m}} := \max_{i,k} \left\| D^{-1}_{\boldsymbol{y}_i^k(H/2, \tau/2)} \big(\boldsymbol{y}^{\mathrm{sem}}(x_i, t^k) - \boldsymbol{y}^{\mathrm{alg}}(x_i) \big) \right\|_\infty,$$

with $D_{\boldsymbol{x}} := \mathrm{diag}(\boldsymbol{x})$. Using the triangle inequality, we have

$$\eta^{\mathrm{m}} \le \max_{i,k} \big(\big\| D^{-1}_{\boldsymbol{y}_i^k(H/2, \tau/2)} \big(\boldsymbol{y}^{\mathrm{sem}}(x_i, t^k) - \boldsymbol{y}_i^k(H/2, \tau/2) \big) \big\|_\infty$$
$$+ \big\| D^{-1}_{\boldsymbol{y}_i^k(H/2, \tau/2)} \big(\boldsymbol{y}_i^k(H/2, \tau/2) - \boldsymbol{y}^{\mathrm{alg}}(x_i) \big) \big\|_\infty \big). \qquad (54)$$

The term $\boldsymbol{y}^{\mathrm{sem}}(x_i, t^k) - \boldsymbol{y}_i^k(H/2, \tau/2)$ in (54) denotes the discretization error of the semilinear model at the gridpoint (x_i, t^k). We note that the right-hand side of the semilinear model in (8) is only once continuously differentiable in both space and time due to the term $q|q|$. Thus, in general, the maximum attainable convergence order in space and time for finite difference schemes is one. However, if q does not change sign during the simulation, i.e., if no backflow occurs, which we assume in the following, then higher order convergence rates can be achieved. Suppose that the discretization scheme for the semilinear model converges with order γ in space and order δ in time. Then, the discretization error has an asymptotic expansion of the form

$$\boldsymbol{y}^{\mathrm{sem}}(x_i, t^k) - \boldsymbol{y}_i^k(H/2, \tau/2) = e(x_i, t^k) \big((H/2)^\gamma + (\tau/2)^\delta \big) + O\big(H^{\gamma+1} + \tau^{\delta+1} \big),$$

with coefficient function $e(x, t)$ that is independent of H and τ, cf. [42]. Hence, we have the first order approximations

$$\boldsymbol{y}^{\mathrm{sem}}(x_i, t^k) - \boldsymbol{y}_i^k(H/2, \tau/2) \doteq e(x_i, t^k) \big((H/2)^\gamma + (\tau/2)^\delta \big), \qquad (55)$$
$$\boldsymbol{y}^{\mathrm{sem}}(x_i, t^k) - \boldsymbol{y}_i^k(H, \tau) \doteq e(x_i, t^k) \big(H^\gamma + \tau^\delta \big). \qquad (56)$$

Subtracting (55) from (56) and rewriting yields

$$e(x_i, t^k) \doteq \frac{\boldsymbol{y}_i^k(H, \tau) - \boldsymbol{y}_i^k(H/2, \tau/2)}{H^\gamma + \tau^\delta - (H/2)^\gamma - (\tau/2)^\delta}.$$

Inserting this into (55) and inserting (55) into (54) results in the first order upper bound for the relative model error

$$
\eta^{\mathrm{m}} \overset{\cdot}{\leq} \max_{i,k} \Big(\frac{(H/2)^{\gamma} + (\tau/2)^{\delta}}{H^{\gamma} + \tau^{\delta} - (H/2)^{\gamma} - (\tau/2)^{\delta}}
$$
$$
\cdot \big\| D^{-1}_{\boldsymbol{y}^k_i(H/2,\tau/2)} \big(\boldsymbol{y}^k_i(H,\tau) - \boldsymbol{y}^k_i(H/2,\tau/2) \big) \big\|_{\infty}
$$
$$
+ \big\| D^{-1}_{\boldsymbol{y}^k_i(H/2,\tau/2)} \big(\boldsymbol{y}^k_i(H/2,\tau/2) - \boldsymbol{y}^{\mathrm{alg}}(x_i) \big) \big\|_{\infty} \Big). \qquad (57)
$$

In order to apply this result, we discretize the semilinear model with the 1S-scheme from subsection 4.1. This discretization scheme is consistent of order 1 both in space and time. The stability of the 1S-scheme is secured by the use of the implicit Euler method in time. Hence, we have convergence of order 1 in space and time, i.e., $\gamma = \delta = 1$. Using e.g. the concrete values $p_{\mathrm{in}} = 5.06 \cdot 10^6$ Pa, $q = 300 \, \mathrm{kg \, s}^{-1}$ for the algebraic model and the values in (37) for the semilinear model, we compute the discrete semilinear solutions $\boldsymbol{y}^k_i(H,\tau)$, $\boldsymbol{y}^k_i(H/2,\tau/2)$ and the algebraic solution $\boldsymbol{y}^{\mathrm{alg}}(x_i)$. From (57), this results for these concrete data in $\eta^{\mathrm{m}} \overset{\cdot}{\leq} 1.16\,\%$.

Having analyzed different error sources for the semilinear model, in the next section we step down one level in the model hierarchy in Figure 2 and perform a similar analysis for the algebraic model.

5 Error Analysis for the Algebraic Model

In this section an error analysis is performed for the temperature dependent algebraic model in (10). This analysis is performed both in terms of backward and forward errors, resulting in first order upper error bounds, in subsection 5.1 and statistically, yielding mean error estimates, in subsection 5.2. Furthermore, it is analyzed in subsection 5.3 under which condition the temperature dependent model can safely be simplified to the isothermal algebraic model. Further details and examples can be found in [43].

5.1 Deterministic Error Analysis

In this subsection a backward error analysis is performed for the algebraic model (10). The rounding errors due to finite precision arithmetic and the uncertainties in the data are interpreted as perturbations in the input parameters. Then, the relative errors in the output parameters are calculated using the individual relative condition numbers and their magnitudes are analyzed for certain concrete input parameter values.

In the equation for the mass flux

$$
\hat{q}(\boldsymbol{d}) = \rho_{\mathrm{in}} v_{\mathrm{in}}, \qquad (58)
$$

which is constant in space, only one multiplication is performed with relative error ε_1, which yields

$$
\begin{aligned}
\tilde{\hat{q}}(\rho_{\text{in}}, v_{\text{in}}) &= \rho_{\text{in}}(1 + \varepsilon_{\rho_{\text{in}}})v_{\text{in}}(1 + \varepsilon_{v_{\text{in}}})(1 + \varepsilon_1) \\
&= \rho_{\text{in}} v_{\text{in}}(1 + \varepsilon_{\rho_{\text{in}}} + \varepsilon_{v_{\text{in}}} + \varepsilon_1 + O(\varepsilon^2)) \\
&= \hat{q}(\rho_{\text{in}}, v_{\text{in}}(1 + \varepsilon_2)),
\end{aligned}
\tag{59}
$$

with $\varepsilon_2 = \varepsilon_{\rho_{\text{in}}} + \varepsilon_{v_{\text{in}}} + \varepsilon_1 + O(\varepsilon^2)$. Here, $\varepsilon_{\rho_{\text{in}}}$ is the relative measurement error in ρ_{in}, $\varepsilon_{v_{\text{in}}}$ the relative data error in v_{in}, and $|\varepsilon_1| < \mathbf{u}$ the relative error of the multiplication, with $\mathbf{u}$ the rounding unit in finite precision arithmetic. For the absolute relative error in $\hat{q}$, using (59), we obtain

$$
\begin{aligned}
\frac{|\hat{q}(\boldsymbol{d}) - \hat{q}(\boldsymbol{d} + \Delta\boldsymbol{d})|}{|\hat{q}(\boldsymbol{d})|} &\leq \left| \frac{\partial \hat{q}}{\partial \rho_{\text{in}}} \frac{1}{\hat{q}(\boldsymbol{d})} \underbrace{\Delta\rho_{\text{in}}}_{0} \right| + \left| \frac{\partial \hat{q}}{\partial v_{\text{in}}} \frac{1}{\hat{q}(\boldsymbol{d})} \Delta v_{\text{in}} \right| + O\left((\Delta\boldsymbol{d})^2\right) \\
&= \left| \underbrace{\left(\frac{\partial \hat{q}}{\partial v_{\text{in}}} \frac{v_{\text{in}}}{\hat{q}(\boldsymbol{d})} \right)}_{\frac{\rho_{\text{in}} v_{\text{in}}}{\rho_{\text{in}} v_{\text{in}}} = 1} \underbrace{\frac{\Delta v_{\text{in}}}{v_{\text{in}}}}_{\varepsilon_2} \right| + O\left((\Delta\boldsymbol{d})^2\right) \\
&= |\varepsilon_2| + \text{h.o.t.} \leq |\varepsilon_{\rho_{\text{in}}}| + |\varepsilon_{v_{\text{in}}}| + |\varepsilon_1| + \text{h.o.t.},
\end{aligned}
$$

where h.o.t. stands for higher order terms in the ε_j. Assuming that the round-off error ε_1 is so small that it can be neglected in comparison with errors $\varepsilon_{\rho_{\text{in}}}$ and $\varepsilon_{v_{\text{in}}}$, then we have the constraint

$$
|\varepsilon_{\rho_{\text{in}}}| + |\varepsilon_{v_{\text{in}}}| \overset{.}{\leq} e_{\text{lim}},
$$

where e_{lim} is a limit for the relative error in $\hat{q}$.

For the computation of the pressure

$$
p(\boldsymbol{d}) = \sqrt{p_{\text{in}}^2 - \frac{\lambda c^2}{2r} \rho v |\rho v|(x - x_0)}
\tag{60}
$$

we use Algorithm 1. Using the Taylor series expansion $\frac{1}{1 - \varepsilon} = 1 + \varepsilon + O(\varepsilon^2)$, this leads to a backward error due to roundoff errors in finite precision arithmetic with unit roundoff $\mathbf{u}$, given by

$$
\tilde{p}(\boldsymbol{d}) = \sqrt{(p_{\text{in}}(1 + \varepsilon_{13}))^2 - \frac{\lambda(1 + \varepsilon_{14})c^2}{2r} \rho v |\rho v|(x - x_0)},
\tag{61}
$$

where

$$
2|\varepsilon_{13}| = |\varepsilon_1 + \varepsilon_{11} + 2\varepsilon_{12} + O(\varepsilon^2)| \leq 4\mathbf{u} + O(\mathbf{u}^2),
$$

so that $|\varepsilon_{13}| \leq 2\mathbf{u} + O(\mathbf{u}^2)$ and $|\varepsilon_{14}| \leq 13\mathbf{u} + O(\mathbf{u}^2)$. Introducing relative data errors and denoting the relative measurement error for the parameter α by ε_α, continuing with (61), gives

$$\tilde{p}(\boldsymbol{d})^2 = \big(p_{\text{in}}(1 + \varepsilon_{15})\big)^2 - \frac{\lambda(1 + \varepsilon_{16})c^2}{2r}\rho v|\rho v|\big(x(1 + \varepsilon_x) - x_0(1 + \varepsilon_{x_0})\big),$$

with

$$|\varepsilon_{15}| = |\varepsilon_{p_{\text{in}}} + \varepsilon_{13} + O(\varepsilon^2)| \leq |\varepsilon_{p_{\text{in}}}| + 2\mathbf{u} + \text{h.o.t.}, \tag{62a}$$

$$|\varepsilon_{16}| \leq |\varepsilon_\lambda| + 2|\varepsilon_c| + |\varepsilon_r| + 2|\varepsilon_\rho| + 2|\varepsilon_v| + 13\mathbf{u} + \text{h.o.t.} \tag{62b}$$

Thus, for the backward error of $p(\boldsymbol{d})$, considered as a function of $p_{\text{in}}, \lambda, x, x_0$, we have the expression

$$\tilde{p}(p_{\text{in}}, \lambda, x, x_0) = p\big(p_{\text{in}}(1 + \varepsilon_{15}), \lambda(1 + \varepsilon_{16}), x(1 + \varepsilon_x), x_0(1 + \varepsilon_{x_0})\big). \tag{63}$$

The effect of the rounding errors in the arithmetic computation of the pressure, given by $2\mathbf{u}$ and $13\mathbf{u}$ in (62), is in general much smaller than the measurement errors for the input parameters, which, in the worst case scenario, can be in the order of a few percent. Hence, the magnitudes of the relative backward errors $\varepsilon_{15}, \varepsilon_{16}, \varepsilon_x, \varepsilon_{x_0}$ mainly depend on the inflicted measurement errors. Using Taylor series expansion and the triangle inequality, it follows from (63) that an upper bound for the relative error in $p(\boldsymbol{d})$ due to the relative perturbations

---

Algorithm 1 : Computing the pressure p in (60)

Input: $p_{\text{in}}, \lambda, c, r, \rho, v, x, x_0$

1: $z_1 \leftarrow p_{\text{in}} \cdot p_{\text{in}}$
2: $z_2 \leftarrow c \cdot c$
3: $z_3 \leftarrow \lambda \cdot z_2$
4: $z_4 \leftarrow 2 \cdot r$
5: $z_5 \leftarrow z_3/z_4$
6: $z_6 \leftarrow \rho \cdot v$
7: $z_7 \leftarrow x - x_0$
8: $z_8 \leftarrow z_5 \cdot z_6$
9: $z_9 \leftarrow z_8 \cdot |z_6|$
10: $z_{10} \leftarrow z_9 \cdot z_7$
11: $z_{11} \leftarrow z_1 - z_{10}$
12: $z_{12} \leftarrow \sqrt{z_{11}}$
13: $p(\boldsymbol{d}) \leftarrow z_{12}$

Output: p

in the data $\boldsymbol{d} = [p_{\text{in}}, \lambda, x, x_0]^T$ caused by rounding and data uncertainty is given by

$$
\frac{|p(\boldsymbol{d}) - p(\boldsymbol{d} + \Delta\boldsymbol{d})|}{p(\boldsymbol{d})} \leq \sum_{i=1}^{4} \left| \frac{\partial p(\boldsymbol{d})}{\partial d_i} \frac{d_i}{p(\boldsymbol{d})} \right| \left| \frac{\Delta d_i}{d_i} \right| + O\left((\Delta\boldsymbol{d})^2\right)
$$

$$
= \underbrace{\left(\frac{p_{\text{in}}}{p(\boldsymbol{d})}\right)^2}_{\kappa_{\text{rel}}(p; p_{\text{in}})} |\varepsilon_{15}| + \underbrace{\frac{\lambda c^2 \rho^2 v^2 (x - x_0)}{4 r p(\boldsymbol{d})^2}}_{\kappa_{\text{rel}}(p; \lambda)} |\varepsilon_{16}| + \underbrace{\frac{\lambda c^2 \rho^2 v^2 |x|}{4 r p(\boldsymbol{d})^2}}_{\kappa_{\text{rel}}(p; x)} |\varepsilon_x|
$$

$$
+ \underbrace{\frac{\lambda c^2 \rho^2 v^2 |x_0|}{4 r p(\boldsymbol{d})^2}}_{\kappa_{\text{rel}}(p; x_0)} |\varepsilon_{x_0}| + \text{h.o.t.}, \tag{64}
$$

where $\kappa_{\text{rel}}(p; p_{\text{in}}), \kappa_{\text{rel}}(p; \lambda), \kappa_{\text{rel}}(p; x), \kappa_{\text{rel}}(p; x_0)$ are the individual relative condition numbers, see (11), which amplify the relative backward errors. Note that the relative condition number $\kappa_{\text{rel}}(p; \boldsymbol{d})$ of p with respect to $\boldsymbol{d}$ is given by the sum of these four individual condition numbers, see (12). Suppose that we require $\kappa_{\text{rel}}(p; p_{\text{in}}) \leq \text{tol}$, where tolerance tol > 1 should depend on $\varepsilon_{p_{\text{in}}}$, then the inequality

$$
\frac{p_{\text{in}}^2}{p_{\text{in}}^2 - \lambda c^2 \rho v |\rho v| (x - x_0)/(2r)} \leq \text{tol}
$$

is obtained. By rewriting this relation it follows that if $\rho v > 0$, then the algebraic model can be used safely for a maximum pipeline length

$$
L = x - x_0 \leq \frac{2 r p_{\text{in}}^2 (1 - 1/\text{tol})}{\lambda c^2 \rho^2 v^2}. \tag{65}
$$

If $\rho v \leq 0$, then there is no such restriction on the pipeline length. Choosing e.g. the concrete nominal values $\boldsymbol{d}_{\text{nom}}$ given by

$$
p_{\text{in}_{\text{nom}}} = 2 \cdot 10^5 \, \text{Pa}, \quad \lambda_{\text{nom}} = 0.03, \quad c_{\text{nom}} = 343 \, \text{m s}^{-1}, \tag{66a}
$$

$$
r_{\text{nom}} = 0.5 \, \text{m}, \quad \rho_{\text{nom}} = 1 \, \text{kg m}^{-3}, \quad v_{\text{nom}} = 10 \, \text{m s}^{-1}, \quad x_{0_{\text{nom}}} = 0 \, \text{m}, \tag{66b}
$$

then $\kappa_{\text{rel}}(p; x) = \kappa_{\text{rel}}(p; \lambda)$ and $\kappa_{\text{rel}}(p; x_0) = 0$. The relative condition numbers $\kappa_{\text{rel}}(p; p_{\text{in}}), \kappa_{\text{rel}}(p; \lambda), \kappa_{\text{rel}}(p; x)$ grow quickly with the pipeline length $L = x - x_0$, see Figure 5. The graphs have a vertical asymptote at $L = 113 \, \text{km}$. Given that we require that $\|[\kappa_{\text{rel}}(p; p_{\text{in}}), \kappa_{\text{rel}}(p; \lambda)]^T\|_\infty \leq 2$, it can be concluded for these concrete data that the algebraic model can only be used safely for pipelines up to 60 km length.

For the computation of the temperature

$$
T(\boldsymbol{d}) = (T_{\text{in}} - T_w) e^{-\frac{k_w}{D c_v \rho v}(x - x_0)} + T_w, \tag{67}
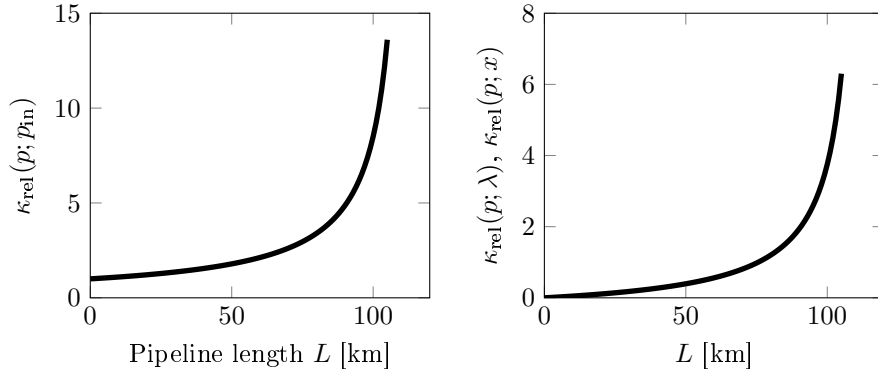$$

Figure 5: The individual relative condition numbers $\kappa_{\mathrm{rel}}(p; p_{\mathrm{in}}), \kappa_{\mathrm{rel}}(p; \lambda)$, $\kappa_{\mathrm{rel}}(p; x)$ in (64) considered as a function of the pipeline length $L = x - x_0$, with the nominal values in (66). The curve $\kappa_{\mathrm{rel}}(p; x)$ is behind the curve $\kappa_{\mathrm{rel}}(p; \lambda)$.

we apply Algorithm 2. Due to rounding errors in finite precision arithmetic, a relative error ε is committed in every step of the algorithm. Using Taylor series expansion, we obtain

$$
\tilde{T}(\boldsymbol{d}) = \Big(T_{\mathrm{in}} \big(1 + \varepsilon_{11} - T_w(\varepsilon_{11} - \varepsilon_{10})/T_{\mathrm{in}} \big) - T_w(1 + \varepsilon_{10}) \Big) e^{-\frac{k_w(1 + \varepsilon_{12})}{D c_v \rho v}(x - x_0)}
$$
$$
+ T_w(1 + \varepsilon_{10}),
$$

Algorithm 2 Computing the temperature T in (67)

Input: T_{in}, T_w, k_w, D, c_v, ρ, v, x, x_0

  1: $z_1 \leftarrow T_{\mathrm{in}} - T_w$
  2: $z_2 \leftarrow D \cdot c_v$
  3: $z_3 \leftarrow z_2 \cdot \rho$
  4: $z_4 \leftarrow z_3 \cdot v$
  5: $z_5 \leftarrow k_w / z_4$
  6: $z_6 \leftarrow x - x_0$
  7: $z_7 \leftarrow z_5 \cdot z_6$
  8: $z_8 \leftarrow e^{-z_7}$
  9: $z_9 \leftarrow z_1 \cdot z_8$
 10: $z_{10} \leftarrow z_9 + T_w$
 11: $T(\boldsymbol{d}) \leftarrow z_{10}$

Output: T

---

where

$$|\varepsilon_{10}| \leq \mathbf{u}, \tag{68a}$$

$$|\varepsilon_{11}| = |\varepsilon_1 + \varepsilon_8 + \varepsilon_9 + \varepsilon_{10} + O(\varepsilon^2)| \leq 4\mathbf{u} + O(\mathbf{u}^2), \tag{68b}$$

$$|\varepsilon_{12}| = |\varepsilon_2 + \varepsilon_3 + \varepsilon_4 + \varepsilon_5 + \varepsilon_6 + \varepsilon_7 + O(\varepsilon^2)| \leq 6\mathbf{u} + O(\mathbf{u}^2). \tag{68c}$$

Including data errors for the input parameters gives

$$\tilde{T}(\boldsymbol{d}) = \left(T_{\text{in}}(1+\varepsilon_{13}) - T_w(1+\varepsilon_{14})\right) e^{-\frac{k_w(1+\varepsilon_{15})}{Dc_v\rho v}\left(x(1+\varepsilon_x) - x_0(1+\varepsilon_{x_0})\right)} + T_w(1+\varepsilon_{14}),$$

with

$$1 + \varepsilon_{13} = 1 + \varepsilon_{T_{\text{in}}} + \varepsilon_{11} - T_w(\varepsilon_{11} - \varepsilon_{10})/T_{\text{in}} + O(\varepsilon^2),$$

$$1 + \varepsilon_{14} = (1 + \varepsilon_{T_w})(1 + \varepsilon_{10}) = 1 + \varepsilon_{T_w} + \varepsilon_{10} + O(\varepsilon^2),$$

$$1 + \varepsilon_{15} = 1 + \varepsilon_{k_w} + \varepsilon_{12} + \varepsilon_D + \varepsilon_{c_v} + \varepsilon_\rho + \varepsilon_v + O(\varepsilon^2).$$

This results in the backward error

$$\begin{aligned}\tilde{T}(T_{\text{in}}, T_w, k_w, x, x_0)\\ = T\left(T_{\text{in}}(1+\varepsilon_{13}), T_w(1+\varepsilon_{14}), k_w(1+\varepsilon_{15}), x(1+\varepsilon_x), x_0(1+\varepsilon_{x_0})\right). \end{aligned} \tag{69}$$

The effect of rounding errors in the computation of the temperature, given by $\mathbf{u}$, $4\mathbf{u}$, $6\mathbf{u}$ in (68), can in general be neglected again as compared to the measurement errors. Thus, for the backward errors it holds that $\varepsilon_{13} \approx \varepsilon_{T_{\text{in}}}$, $\varepsilon_{14} \approx \varepsilon_{T_w}$, $\varepsilon_{15} \approx \varepsilon_{k_w} + \varepsilon_D + \varepsilon_{c_v} + \varepsilon_\rho + \varepsilon_v$. From (69) it follows that an upper bound for the relative error in the temperature $T(\boldsymbol{d})$ due to finite precision arithmetic and data errors is given by

$$\begin{aligned}\frac{|\Delta T|}{T(\boldsymbol{d})} \leq &\underbrace{\frac{T_{\text{in}}}{\left|T_{\text{in}} + \left(e^{\frac{k_w(x-x_0)}{Dc_v\rho v}} - 1\right)T_w\right|}}_{\kappa_{\text{rel}}(T;T_{\text{in}})}|\varepsilon_{13}| + \underbrace{\left|\frac{T_w - T_w e^{-\frac{k_w(x-x_0)}{Dc_v\rho v}}}{(T_{\text{in}} - T_w)e^{-\frac{k_w(x-x_0)}{Dc_v\rho v}} + T_w}\right|}_{\kappa_{\text{rel}}(T;T_w)}|\varepsilon_{14}|\\ &+ \underbrace{\left|\frac{(T_{\text{in}} - T_w)(x-x_0)k_w}{Dc_v\rho v\left(T_{\text{in}} + (e^{\frac{k_w(x-x_0)}{Dc_v\rho v}} - 1)T_w\right)}\right|}_{\kappa_{\text{rel}}(T;k_w)}|\varepsilon_{15}|\\ &+ \underbrace{\left|\frac{(T_{\text{in}} - T_w)k_w x}{Dc_v\rho v T(\boldsymbol{d})}\right| e^{-\frac{k_w(x-x_0)}{Dc_v\rho v}}}_{\kappa_{\text{rel}}(T;x)}|\varepsilon_x|\end{aligned}$$

$$+ \underbrace{\left| \frac{(T_{\text{in}} - T_w)k_w x_0}{Dc_v \rho v T(\boldsymbol{d})} \right| e^{-\frac{k_w(x-x_0)}{Dc_v \rho v}}}_{\kappa_{\text{rel}}(T;x_0)} |\varepsilon_{x_0}| + O\left((\Delta \boldsymbol{d})^2\right), \tag{70}$$

with $\Delta T = T(\boldsymbol{d}) - T(\boldsymbol{d} + \Delta \boldsymbol{d})$. To see whether the relative backward errors $|\varepsilon_{13}|, |\varepsilon_{14}|, |\varepsilon_{15}|, |\varepsilon_x|, |\varepsilon_{x_0}|$ are amplified in the relative error for the temperature, we consider e.g. the concrete nominal values

$$D_{\text{nom}} = 1\,\text{m}, \quad \rho_{\text{nom}} = 1\,\text{kg}\,\text{m}^{-3}, \quad v_{\text{nom}} = 10\,\text{m}\,\text{s}^{-1}, \quad T_{\text{in}_{\text{nom}}} = 293\,\text{K}, \tag{71a}$$

$$T_{w_{\text{nom}}} = 283\,\text{K}, \quad k_{w_{\text{nom}}} = 0.0341\,\text{W}\,\text{m}^{-1}\,\text{K}^{-1}, \tag{71b}$$

$$c_{v_{\text{nom}}} = 1700\,\text{J}\,\text{kg}^{-1}\,\text{K}^{-1}, \quad x_{0_{\text{nom}}} = 0\,\text{m}, \tag{71c}$$

in the individual relative condition numbers in (70). With $x_{0_{\text{nom}}} = 0$, then $\kappa_{\text{rel}}(T;x_0) = 0$. The four remaining relative condition numbers are depicted in Figure 6 as a function of the pipeline length $L = x - x_0$. The figure shows that all condition numbers remain below one, which means that the relative errors in the input parameters are not amplified. The relative condition numbers $\kappa_{\text{rel}}(T;k_w), \kappa_{\text{rel}}(T;x)$ are so small as compared to $\kappa_{\text{rel}}(T;T_{\text{in}}), \kappa_{\text{rel}}(T;T_w)$ that they can be neglected. Again, we note that the relative condition number $\kappa_{\text{rel}}(T;\boldsymbol{d})$ of T with respect to $\boldsymbol{d} = [T_{\text{in}}, T_w, k_w, x, x_0]^T$ is given by the sum of the four individual condition numbers.

Our backward analysis and the computation of the associated condition numbers show that the values for the pressure are most affected by data and rounding errors and present restrictions to the pipeline length that can be safely considered. This theoretical analysis presents a first order worst case error analysis. >From a practical point of view the worst case analysis is important to obtain warnings, but in view of the large uncertainty that the data will have a statistical analysis, which results in average perturbation estimates, seems more adequate. Such an analysis is performed in the next subsection.

5.2 Statistical Perturbation Analysis

In this subsection we compute average perturbation amplification estimates for the algebraic model (10) using a statistical analysis. It complements the theoretical worst case analysis carried out in the previous subsection.

The efficient URQ method, see subsection 3.2, enables us to calculate the relative standard deviation of the pressure p and the temperature T for many different pipeline lengths L. The mean of the remaining input parameters is set to the nominal values in (66), (71). The relative standard deviation σ_{d_i}/μ_{d_i} is set to 0.5 % for every input parameter d_i of $\boldsymbol{d}$. Subsequently, the mean perturbation amplification factors $\phi(p;\boldsymbol{d}), \phi(T;\boldsymbol{d})$, see (32), are computed as
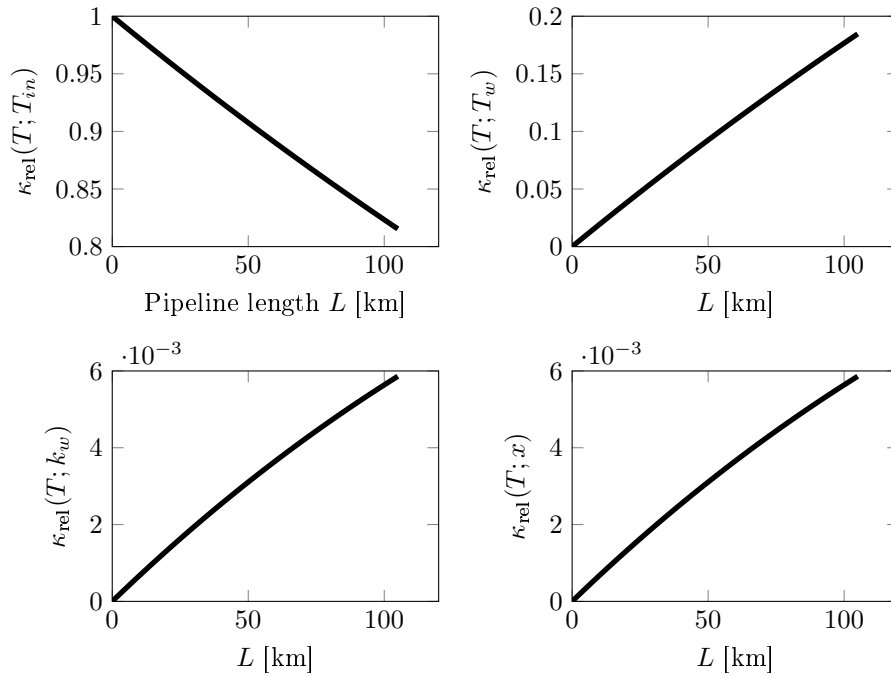
Figure 6: The individual relative condition numbers $\kappa_{\mathrm{rel}}(T; T_{\mathrm{in}})$, $\kappa_{\mathrm{rel}}(T; T_w)$, $\kappa_{\mathrm{rel}}(T; k_w)$, $\kappa_{\mathrm{rel}}(T; x)$ in (70) considered as a function of the pipeline length $L = x - x_0$ for the concrete values in (71).

a function of L. The average perturbation amplification results of the URQ simulation for p and T are depicted in Figure 7. A similar behavior as in the worst case analysis in subsection 5.1 is observed; the uncertainty in the pressure grows quickly for increasing pipeline length and the uncertainty in the temperature decreases slightly for increasing L. As expected, the average uncertainty amplification factors $\phi(p; \boldsymbol{d}), \phi(T; \boldsymbol{d})$ in Figure 7 are smaller than the first order upper bounds $\kappa_{\mathrm{rel}}(p; \boldsymbol{d}), \kappa_{\mathrm{rel}}(T; \boldsymbol{d})$, which are obtained by taking the sum of the individual condition numbers in Figures 5 and 6, see (12). The mass flux $\hat{q}$ is not considered here, because it is constant with respect to L.

Concluding, the backward errors due to rounding and data uncertainty have been presented in the previous subsection. Multiplying these backward errors with the condition numbers from subsection 5.1 results in first order worst case error bounds. On the other hand, multiplying the backward errors with the average amplification factors given in this subsection, yields mean
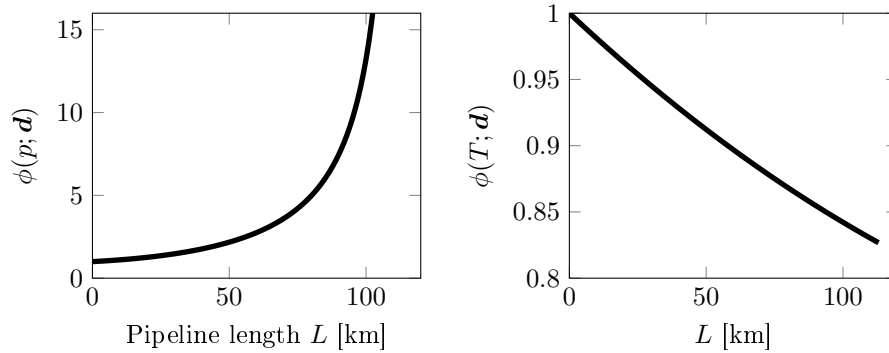
Figure 7: The mean uncertainty amplification factors ϕ, see (32), for the pressure p (left) and the temperature T (right) as a function of the pipeline length L, computed with the URQ method. The relative standard deviation of the input parameters is set to $0.5\,\%$ with mean values in (66), (71).

error estimates. The worst case bounds and the mean estimates together provide a useful description of the error in the pressure and the temperature due to rounding and data uncertainty.

Having performed the analysis for the algebraic model including temperature and having observed that the temperature dependence is rather insensitive, we can also extend the simplification of the algebraic model to the isothermal version by assuming the temperature T to be constant. The error inflicted by this simplification is analyzed in the following subsection.

5.3 Error between Temperature Dependent and Isothermal Algebraic Model

In this subsection we analyze the error that is committed when the temperature dependent algebraic model in (10) is simplified to the isothermal algebraic model in (10a), (10b), see the lower level of the model hierarchy in Figure 2.

Suppose that the temperature in the algebraic model is set constant and that the value $T(\boldsymbol{d})$, for certain parameter values $\boldsymbol{d}$, is taken for this constant temperature, whereas the actual parameter values are given by $\tilde{\boldsymbol{d}}$. Then, using Taylor series expansion and the triangle inequality, a first order upper bound for the relative error in T is given by

$$\frac{|T(\boldsymbol{d}) - T(\tilde{\boldsymbol{d}})|}{|T(\boldsymbol{d})|} \dot{\leq} \sum_{i=1}^{n} \left| \frac{\partial T(\boldsymbol{d})}{\partial d_i} \frac{d_i}{T(\boldsymbol{d})} \right| \frac{|d_i - \tilde{d}_i|}{|d_i|}.$$

Inserting the nominal values $\boldsymbol{d}_{\text{nom}}$ in (71) together with $x_{\text{nom}} = 70\,\text{km}$, the individual relative condition numbers for T with respect to the parameter vector $\boldsymbol{d}$ are given by

$$
\left| \frac{\partial T(\boldsymbol{d})}{\partial \rho} \frac{\rho}{T(\boldsymbol{d})} \right| = \left| \frac{\partial T(\boldsymbol{d})}{\partial v} \frac{v}{T(\boldsymbol{d})} \right| = \left| \frac{\partial T(\boldsymbol{d})}{\partial D} \frac{D}{T(\boldsymbol{d})} \right| = \left| \frac{\partial T(\boldsymbol{d})}{\partial x} \frac{x}{T(\boldsymbol{d})} \right|
$$
$$
= \left| \frac{\partial T(\boldsymbol{d})}{\partial k_w} \frac{k_w}{T(\boldsymbol{d})} \right| = \left| \frac{\partial T(\boldsymbol{d})}{\partial c_v} \frac{c_v}{T(\boldsymbol{d})} \right| = 4.18 \cdot 10^{-3},
$$
$$
\left| \frac{\partial T(\boldsymbol{d})}{\partial x_0} \frac{x_0}{T(\boldsymbol{d})} \right| = 0, \quad \left| \frac{\partial T(\boldsymbol{d})}{\partial T_{\text{in}}} \frac{T_{\text{in}}}{T(\boldsymbol{d})} \right| = 8.73 \cdot 10^{-1},
$$
$$
\left| \frac{\partial T(\boldsymbol{d})}{\partial T_w} \frac{T_w}{T(\boldsymbol{d})} \right| = 1.27 \cdot 10^{-1}.
$$

It follows that only perturbations in the parameter T_{in} create an equivalent relative perturbation in the temperature T. Perturbations in the other input parameters only cause a small relative error in T. This means that if the input temperature T_{in} is not subject to change, then the temperature can safely be set constant. If, however, the input temperature changes, for example for different pipelines, then the temperature cannot be set constant and the temperature dependent algebraic model should be chosen.

6   Conclusions and Outlook

This paper presents an error and perturbation analysis for the Euler equations in semilinear and algebraic form. The main focus is on the effect of rounding and data uncertainty errors on the solution of these two models. However, also the modeling error that is committed in the different simplifications, the discretization error for the semilinear model, and the iteration error due to a preliminary stopping of the Newton method are analyzed.

The partial differential equations of the semilinear model are discretized by applying two simple schemes which are used in natural gas network optimization problems. It is shown that the normwise relative condition number of the resulting nonlinear systems leads to a considerable overestimation of the sensitivity of the problems. The novel componentwise relative condition number constitutes a more accurate measure for the sensitivity. Furthermore, it is shown that the mass flow rate has higher condition numbers with respect to the uncertain parameters than the pressure and we can determine stepsizes for which well-conditioned problems are obtained. Moreover, it is shown that the rounding and iteration errors can be neglected compared to the data uncertainty error and we find that the modeling error between the semilinear

and the algebraic model is approximately 1% for certain concrete parameter values.

The error analysis for the pressure in the algebraic model results in a rounding and data uncertainty error that grows quickly with increasing pipeline length, such that the algebraic model can only be used safely for short pipelines (for certain parameter values up to 60 km length). The error in the temperature decreases slightly with increasing pipeline length. These results are obtained both via a deterministic first order worst case and via a statistical mean perturbation analysis. Finally, it is shown that only if the pipeline input temperature is not subject to change, then the temperature can safely be set constant and the isothermal algebraic model can be used.

Future work will implement the derived error estimators into a robust error controller, which allows to adaptively switch between different simulation models within the gas pipeline network in order to achieve a prescribed accuracy while minimizing the computational cost.

References

[1] Bundesministerium für Wirtschaft und Energie. Primärenergieverbrauch nach Energieträgern. `http://www.bmwi.de`. Accessed: 2016-04-19.

[2] M.A. Adewumi and J. Zhou. Simulation of transient flow in natural gas pipelines. 27th Annual Meeting of PSIG (Pipeline Simulation Interest Group), Albuquerque, NM, 1995.

[3] M.K. Banda, M. Herty, and A. Klar. Coupling conditions for gas networks governed by the isothermal Euler equations. *Netw. Heterog. Media*, 1(2):295–314, 2006.

[4] M.K. Banda, M. Herty, and A. Klar. Gas flow in pipeline networks. *Netw. Heterog. Media*, 1(1):41–56, March 2006.

[5] K.S. Chapman, P. Krishniswami, V. Wallentine, M. Abbaspour, R. Ranganathan, R. Addanki, J. Sengupta, and L. Chen. Virtual pipeline system testbed to optimize the U.S. natural gas transmission pipeline system. Technical Report DE-FC26-01NT41322, The National Gas Machinery Laboratory, Kansas State University, 2005.

[6] R.M. Colombo and M. Garavello. A well-posed Riemann problem for the p-system at a junction. *Netw. and Heterog. Media*, 1(3):495–511, 2006.

[7] P. Domschke, O. Kolb, and J. Lang. Adjoint-based error control for the simulation and optimization of gas and water supply networks. *Appl. Math. Comput.*, 259:1003–1018, 2015.

[8] K. Ehrhardt and M.C. Steinbach. KKT systems in operative planning for gas distribution networks. *Proc. Appl. Math. Mech.*, 4(1):606–607, 2004.

[9] K. Ehrhardt and M.C. Steinbach. Nonlinear optimization in gas networks.

In H. G. Bock, E. Kostina, H. X. Phu, and R. Ranacher, editors, *Modeling, Simulation and Optimization of Complex Processes*, pages 139–148. Springer, Berlin Heidelberg, 2005.

[10] M. Herty, J. Mohring, and V. Sachers. A new model for gas flow in pipe networks. *Math. Methods Appl. Sci.*, 33(7):845–855, 2010.

[11] S. L. Ke and H. C. Ti. Transient analysis of isothermal gas flow in pipeline networks. *Chem. Eng. J.*, 76(2):169–177, 2000.

[12] A. Martin, M. Möller, and S. Moritz. Mixed integer models for the stationary case of gas network optimization. *Math. Program.*, 105(2):563–582, 2006.

[13] A.J. Osiadacz and M. Chaczykowski. Comparison of isothermal and non-isothermal pipeline gas flow models. *Chem. Eng. J.*, 81(1–3):41–51, 2001.

[14] M. C. Steinbach. On PDE solution in transient optimization of gas networks. *J. Comput. Appl. Math.*, 203(2):345–361, 2007. Special Issue: The first Indo-German Conference on PDE, Scientific Computing and Optimization in Applications.

[15] M.K. Banda and M. Herty. Multiscale modeling for gas flow in pipe networks. *Math. Methods Appl. Sci.*, 31(8):915–936, 2008.

[16] J. Brouwer, I. Gasser, and M. Herty. Gas pipeline models revisited: Model hierarchies, nonisothermal models, and simulations of networks. *Multiscale Model. Simul.*, 9(2):601–623, 2011.

[17] P. Domschke. *Adjoint-Based Control of Model and Discretization Errors for Gas Transport in Networked Pipelines*. PhD thesis, TU Darmstadt, Verlag Dr. Hut, 2011.

[18] P. Domschke, O. Kolb, and J. Lang. Adjoint-based control of model and discretisation errors for gas and water supply networks. In X. Yang and S. Koziel, editors, *Computational Optimization and Applications in Engineering and Industry*, pages 1–17. Springer, Berlin Heidelberg, 2011.

[19] N.J. Higham. *Accuracy and Stability of Numerical Algorithms*. SIAM, Philadelphia, PA, second edition, 2002.

[20] P. Domschke, O. Kolb, and J. Lang. An adaptive model switching and discretization algorithm for gas flow on networks. *Procedia Comput. Sci.*, 1(1):1331–1340, 2010.

[21] M. Konstantinov, D.W. Gu, V. Mehrmann, and P. Petkov. *Perturbation Theory for Matrix Equations*. Studies in Computational Mathematics. Elsevier Science, North Holland, 2003.

[22] R. Le Veque. *Finite Volume Methods for Hyperbolic Problems*. Cambridge Texts in Applied Mathematics. Cambridge University Press, Cambridge, UK, 2002.

[23] P. Bales. Hierarchische Modellierung der Eulerschen Flussgleichungen in der Gasdynamik. Diplomarbeit, TU Darmstadt, 2005.

[24] M. Schmidt, M.C. Steinbach, and B.M. Willert. High detail stationary optimization models for gas networks. *Optimization and Engineering*, 16(1):131–164, 2015.

[25] International Organization for Standardization. ISO 6976:1995 Natural gas – Calculation of calorific values, density, relative density and Wobbe index from composition. `https://www.iso.org/obp/ui/#iso:std:iso:6976:ed-2:v2:en`, 1995. Accessed: 2016-04-20.

[26] A.J. Osiadacz. *Simulation and analysis of gas networks*. E. & F.N. Spon, London, 1987.

[27] A.J. Osiadacz. Different transient flow models – limitations, advantages, and disadvantages. 28th Annual Meeting of PSIG (Pipeline Simulation Interest Group), San Francisco, CA, 1996.

[28] B. Geißler, A. Martin, A. Morsi, and L. Schewe. Using piecewise linear functions for solving MINLPs. In J. Lee and S. Leyffer, editors, *Mixed Integer Nonlinear Programming*, volume 154 of *The IMA Volumes in Mathematics and its Applications*, pages 287–314. Springer, New York, 2012.

[29] T. Koch, B. Hiller, M.E. Pfetsch, and L. Schewe. *Evaluating Gas Network Capacities*. MOS-SIAM Series on Optimization. SIAM, Philadelphia, PA, 2015.

[30] M. Bollhöfer and V. Mehrmann. *Numerische Mathematik – Eine projektorientierte Einführung für Ingenieure, Mathematiker und Naturwissenschaftler*. vieweg studium; Grundkurs Mathematik. Vieweg+Teubner Verlag, Wiesbaden, 2004.

[31] J.R. Rice. *Numerical Methods, Software, and Analysis*. Academic Press, San Diego, CA, second edition, 1993.

[32] J.H. Wilkinson. *Rounding Errors in Algebraic Processes*. Dover books on advanced mathematics. Dover Publications, New York, NY, 1994.

[33] P. Deuflhard and A. Hohmann. *Numerical analysis, A first course in scientific computation*. De Gruyter Textbook. Walter de Gruyter & Co., Berlin, 1995.

[34] H. Woźniakowski. Numerical stability for solving nonlinear equations. *Numer. Math.*, 27(4):373–390, 1976.

[35] G. Strang. *Linear Algebra and its Applications*. Academic Press, New York, NY, second edition, 1980.

[36] F. Chaitin-Chatelin and V. Frayssé. *Lectures on Finite Precision Computations*. Software, Environments and Tools. SIAM, Philadelphia, PA, 1996.

[37] M. Padulo, M. S. Campobasso, and M. D. Guenov. Novel Uncertainty Propagation Method for Robust Aerodynamic Design. *AIAA Journal*, 49(3):530–543, 2011.

[38] S. Moritz. *A Mixed Integer Approach for the Transient Case of Gas*

Network Optimization. PhD thesis, TU Darmstadt, 2006.

[39] C.T. Kelley. *Iterative Methods for Linear and Nonlinear Equations*. Frontiers in Applied Mathematics. SIAM, Philadelphia, PA, 1995.

[40] O. Kolb, J. Lang, and P. Bales. An implicit box scheme for subsonic compressible flow with dissipative source term. *Numer. Algorithms*, 53(2-3):293–307, 2010.

[41] T. J. Ypma. The effect of rounding errors on Newton-like methods. *IMA J. Numer. Anal.*, 3(1):109–118, 1983.

[42] C. Grossmann and H. Roos. *Numerical treatment of partial differential equations*. Universitext. Springer, Berlin, 2007. Translated and revised from the 3rd (2005) German edition by Martin Stynes.

[43] V. Mehrmann and J.J. Stolwijk. Error analysis for the Euler equations in purely algebraic form. Technical Report 2015/06, TU Berlin, Institut für Mathematik, 2015.

Jeroen J. STOLWIJK,
Institut für Mathematik, MA 4-5,
Technische Universität Berlin,
Str. des 17. Juni 136, D-10623 Berlin, Germany
Email: stolwijk@math.tu-berlin.de

Volker MEHRMANN,
Institut für Mathematik, MA 4-5,
Technische Universität Berlin,
Str. des 17. Juni 136, D-10623 Berlin, Germany
Email: mehrmann@math.tu-berlin.de